ORGANOMETALLICS

ARTICLE

pubs.acs.org/Organometallics

Ferrocenyl Diquat Derivatives: Nonlinear Optical Activity, Multiple Redox States, and Unusual Reactivity

Benjamin J. Coe,*[,†] John Fielden,[†] Simon P. Foxon,[†] Inge Asselberghs,[‡] Koen Clays,[‡] Stijn Van Cleuvenbergen,[‡] and Bruce S. Brunschwig[§]

[†]School of Chemistry, University of Manchester, Oxford Road, Manchester M13 9PL, U.K.

[‡]Department of Chemistry, University of Leuven, Celestijnenlaan 200D, B-3001 Leuven, Belgium

[§]Molecular Materials Research Center, Beckman Institute, MC 139-74, California Institute of Technology, 1200 East California Boulevard, Pasadena, California 91125, United States

Supporting Information

ABSTRACT:

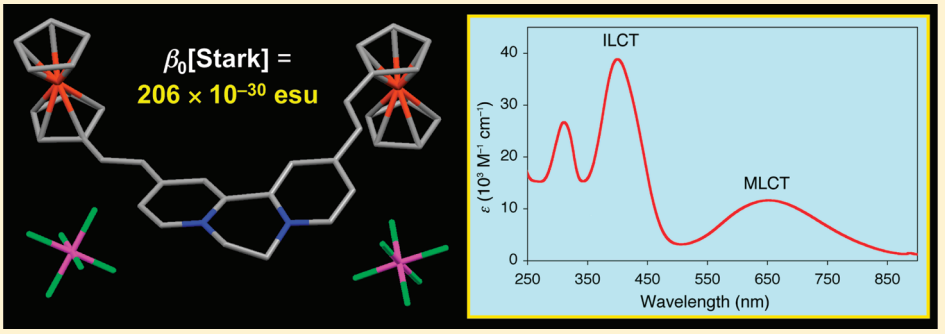

Four new dipolar cations have been synthesized, containing ferrocenyl electron donor groups and diquaternized 2,2′-bipyridyl (diquat) acceptors. To our knowledge, these are the first organometallic diquat derivatives to be reported and have been characterized as their PF_6^- salts by using various techniques including ^{1}H NMR and electronic absorption spectroscopies and cyclic voltammetry. UV−vis spectra show multiple intramolecular charge-transfer bands, and three reversible redox processes are observed for each compound. Molecular quadratic nonlinear optical (NLO) responses have been determined by using hyper-Rayleigh scattering at 1064 nm and Stark (electroabsorption) spectroscopic studies on the intense $\pi \rightarrow \pi^*$ intraligand and $d \rightarrow \pi^*$ metal-to-ligand charge-transfer bands. The most active compounds have estimated, Stark-derived β_0 values approaching that of the chromophore in the technologically important material (*E*)-4′-(dimethylamino)-*N*-methyl-4-stilbazolium tosylate. Single-crystal X-ray structures have been obtained for three of the salts, with one adopting the orthorhombic space group *Aba*2 and having potential for bulk NLO behavior due to its polar structure. Attempted crystallizations of the remaining chromophore revealed that it undergoes an unusual intermolecular formal Michael cycloaddition between an activated methyl group and a double bond, forming a dimeric species. This diastereomeric cyclic complex has also been characterized via single-crystal X-ray diffraction.

INTRODUCTION

Organic nonlinear optical (NLO) materials are of great current interest.[1] As well as academic incentives, research is motivated by applications such as biological imaging and advanced telecommunications, for example the creation of all-optical computing devices. While most of this research has focused on purely organic chromophores, metalloorganic species are also highly attractive.[2] The facility of design associated with organic materials can be combined with metals to introduce additional properties, such as redox chemistry[3] or magnetism (often in hybrid materials).[2c,d,4] In addition, the presence of metal ions can allow the construction of chromophores with unusual shapes, e.g., 3D octupoles,[2g,5] or direct the formation of coordination polymers with NLO activity.[6]

For molecular compounds, quadratic (second-order) NLO behavior arises from the first hyperpolarizability β that translates into the macroscopic coefficient $\chi^{(2)}$ in materials. To achieve nonzero values of both β and $\chi^{(2)}$, noncentrosymmetric structures are essential. Large β responses are generally found in organic and metalloorganic molecules having electron donor (ED) and acceptor (EA) groups linked via polarizable π-systems. Typically, these are simple 1D dipoles, such as the commercially exploited (*E*)-4′-(dimethylamino)-*N*-methyl-4-stilbazolium (DAS^+) cation.[7] However, multidimensional species such as octupoles and 2D dipoles[2c,8] offer potential advantages over their 1D

Received: July 8, 2011
Published: October 12, 2011

counterparts. These include larger NLO responses without sacrificing visible transparency and possibilities to use polarization effects to avoid reabsorption of light produced by the quadratic effect second-harmonic generation (SHG).[8a] The noncentrosymmetry necessary for bulk effects such as SHG or electro-optic behavior may be achieved in crystals, e.g., DAS$^+$ tosylate (DAST),[7] or in other ordered systems such as poled polymers and Langmuir–Blodgett thin films.

Inspired by a seminal report by Green, Marder, and colleagues,[9] many investigations into quadratic NLO properties have exploited the ferrocenyl (Fc) group (or its methylated derivatives) as an electron donor.[2b,10] Although the Fc moiety itself is a weaker π-ED group when compared with an alkylamino unit,[11] methylation enhances its donating strength, and well-defined redox chemistry can be used to switch NLO behavior.[3a,b] In addition, Fc derivatives are highly stable and also amenable to very extensive functionalization chemistry. Besides NLO properties, other motivations for the study of EA-containing Fc derivatives are diverse and encompass photoinduced electron-transfer (including potential applications in dye-sensitized solar cells),[12] ion sensing,[13] electrochromism,[14] and pH-switchable optical properties.[15]

Studies with charged, Fc-containing NLO chromophores have included monometallic species with mostly *N*-methylpyridinium π-EAs[11,16] and various bimetallic complexes.[17] However, despite some promising results, particularly with salts of the cation (*E*)-*N*-methyl-4-[2-(ferrocenyl)vinyl]pyridinium,[16b] the potential of relatively simple salts containing Fc groups remains relatively unexplored. Therefore, we recently reported Fc derivatives with strong *N*-arylpyridinium π-EAs, achieving static first hyperpolarizabilities β_0 of up to 288 $\times$ 10^{-30} esu derived from Stark spectroscopic data.[18] We have also investigated a large family of purely organic chromophores based on diquaternized 2,2′-bipyridyl (diquat, DQ^{2+}) units.[19] Such π-EAs (Figure 1) offer the following attractive features: (i) acceptor strengths higher than that of *N*-alkylpyridinium groups; (ii) two well-separated and reversible reductions; (iii) the ability to connect two π-EDs in V-shaped, 2D species; and (iv) possibilities for tuning structural and electronic properties by changing the length of the quaternizing bridge. Motivated by the goal of creating multistate optical switches, here we present a study of 1D and 2D metallochromophores in which DQ^{2+} groups are linked to redox-active Fc moieties.

EXPERIMENTAL SECTION

Materials and Procedures. Acetonitrile and DCM were dried over CaH_2 and distilled under nitrogen. All other reagents and solvents were obtained as ACS grade from Sigma Aldrich, Alfa Aesar, or Fisher Scientific and used as supplied. The compounds 1,2-bis(triflyloxy)ethane,[20] 1,3-bis(triflyloxy)propane,[20] 4-[(diethoxyphosphinyl)methyl]-4′-methyl-2,2′-bipyridyl,[21a] and 4,4′-bis[(diethoxyphosphinyl)methyl]-2,2′-bipyridyl[21b] were synthesized according to previously published methods. Products were dried at room temperature overnight in a vacuum desiccator ($CaSO_4$) prior to characterization.

General Physical Measurements. ^{1}H NMR spectra were recorded on Bruker UltraShield 500, AV-400, or DPX-300 spectrometers and all shifts are quoted with respect to TMS. The fine splitting of pyridyl or phenyl ring AA′BB′ patterns is ignored, and the signals are reported as simple doublets, with *J* values referring to the two most intense peaks. Where additional peaks due to minor rotamers are observed ($[\mathbf{3}/\mathbf{4}][PF_6]_2$), only the data for the major rotamer are reported in this section. Abbreviations used: ax = axial; eq = equatorial. Elemental analyses were performed by the Microanalytical Laboratory, University of Manchester, using a Carlo Erba EA1108 instrument, and thermogravimetric analyses (TGA) were performed by the same service (heating up to 600 °C under N_2). UV–vis spectra were obtained by using a Shimadzu UV-2401 PC spectrophotometer, and mass spectra were recorded by using +electrospray on a Micromass Platform II spectrometer. Cyclic voltammetric measurements were performed by using an EG&G PAR model 283 or an Autolab PGStat 100 potentiostat/galvanostat. A single-compartment cell was used with a silver/silver chloride reference electrode (3 M NaCl, saturated AgCl) separated by a salt bridge from a 2 mm disk glassy carbon working electrode and Pt wire auxiliary electrode. Acetonitrile was freshly distilled (from CaH_2), and $[NBu^n_4]PF_6$, as supplied from Fluka, was used as the supporting electrolyte. Solutions containing ca. 10^{-3} M analyte (0.1 M electrolyte) were deaerated by purging with nitrogen. All $E_{1/2}$ values were calculated from $(E_{pa} + E_{pc})/2$ at a scan rate of 200 mV s^{-1}.

Synthesis of 4-[(*E*)-2-(Ferrocenyl)vinyl]-4′-methyl-2,2′-bipyridyl, 1. Potassium *tert*-butoxide (97 mg, 0.864 mmol) was added to a stirred solution of 4-[(diethoxyphosphinyl)methyl]-4′-methyl-2,2′-bipyridyl (200 mg, 0.624 mmol) and ferrocenecarboxaldehyde (134 mg, 0.626 mmol) in THF (20 mL). The reaction vessel was sealed and stirred at room temperature for 18 h. Distilled water (20 mL) was added to the deep red mixture, and the THF removed under vacuum. The orange solid was filtered off and washed with water and a small amount of methanol: 179 mg, 74%. ^{1}H NMR (400 MHz, $CDCl_3$): δ 8.64–8.58 (2 H, m, C_5H_3N), 8.50 (1 H, s, C_5H_3N), 8.36 (1 H, s, C_5H_3N), 7.39–7.32 (2 H, C_5H_3N + CH), 7.21 (1 H, d, J = 5.1 Hz, C_5H_3N), 6.73 (1 H, d, J = 16.1 Hz, CH), 4.54 (2 H, t, J = 1.9 Hz, C_5H_4), 4.40 (2 H, t, J = 1.9 Hz, C_5H_4), 4.18 (5 H, s, C_5H_5), 2.46 (3 H, s, Me). Anal. Calcd (%) for $C_{23}H_{20}FeN_2 \cdot 0.33H_2O$: C, 71.53; H, 5.39; N, 7.25. Found: C, 71.48; H, 5.15; N, 6.87. MS: m/z = 381.3 ($[MH]^+$).

Synthesis of 4,4′-Bis[(*E*)-2-(ferrocenyl)vinyl]-2,2′-bipyridyl, 2. Potassium *tert*-butoxide (312 mg, 2.78 mmol) was added to a stirred solution of 4,4′-bis[(diethoxyphosphinyl)methyl]-2,2′-bipyridyl (500 mg, 1.10 mmol) and ferrocenecarboxaldehyde (516 mg, 2.41 mmol) in THF (30 mL). The reaction vessel was sealed and stirred in the dark at room temperature for 4 h. Distilled water (60 mL) was added, and the reaction was stirred for a further few minutes. The orange solid was filtered off and washed with copious amounts of water followed by ethyl acetate and diethyl ether: 584 mg, 93%. The crude product was precipitated from chloroform (300 mL) and pentane (600 mL) to afford a red solid: 503 mg, 79%. ^{1}H NMR (400 MHz, $CDCl_3$): δ 8.63 (2 H, d, J = 5.2 Hz, C_5H_3N), 8.46 (2 H, s, C_5H_3N), 7.31–7.28 (4 H, C_5H_3N + 2CH), 6.73 (2 H, d, J = 16.0 Hz, 2CH), 4.53 (4 H, t, J = 1.9 Hz, $2C_5H_4$), 4.36 (4 H, t, J = 1.9 Hz, $2C_5H_4$), 4.16 (10 H, s, $2C_5H_5$). Anal. Calcd (%) for $C_{34}H_{28}Fe_2N_2 \cdot 0.33H_2O$: C, 70.14; H, 4.96; N, 4.81. Found: C, 70.06; H, 5.15; N, 4.64. MS: m/z = 577.3 ($[MH]^+$). TGA shows a mass loss of ca. 1%, consistent with the loss of ca. 1/3 equivalent of water upon heating to 310 °C.

Synthesis of 2-Methyl-11-[(*E*)-2-(ferrocenyl)vinyl]-6,7-dihydro-dipyrido[1,2-*a*:2′,1′-*c*]pyrazinediium Hexafluorophosphate, [3][PF$_6$]$_2$. A solution of 1,2-bis(triflyloxy)ethane (85 mg, 0.261 mmol) in dry DCM (ca. 1 mL) was added to a stirred solution of $\mathbf{1} \cdot 0.33H_2O$ (50 mg, 0.129 mmol) in dry DCM (10 mL). The orange solution rapidly darkened in color before it was protected from the light and stirred at room temperature for 72 h. The volume was reduced to ca. 5 mL under vacuum, and diethyl ether (20 mL) was added to ensure complete precipitation of crude $[\mathbf{3}][OTf]_2$. This solid was filtered off, then redissolved in a minimum amount of methanol. The product was precipitated by addition of 10% aqueous NH_4PF_6, filtered off, and washed with water. Reprecipitation from acetone/diethyl ether gave a dark green solid: 55 mg, 61%. ^{1}H NMR (400 MHz, $(CD_3)_2CO$): δ 9.30 (1 H, d, J = 6.3 Hz, C_5H_3N), 9.11–9.05 (3 H, C_5H_3N), 8.39 (1 H, d, J = 6.3 Hz, C_5H_3N), 8.35 (1 H, d, J = 6.6 Hz, C_5H_3N), 8.26 (1 H, d, J = 15.9 Hz, CH), 7.18 (1 H, d, J = 15.9 Hz, CH), 5.60–5.55 (2 H, m, CH_2),

Table 1. Crystallographic Data and Refinement Details for the Salts $[3][PF_6]_2\cdot 2Me_2CO$, $[4b][PF_6]_4\cdot 4Me_2CO$, $[5][PF_6]_2\cdot 3Me_2CO$, and $[6][PF_6]_2$

	$[3][PF_6]_2\cdot 2Me_2CO$	$[4b][PF_6]_4\cdot 4Me_2CO$	$[5][PF_6]_2\cdot 3Me_2CO$	$[6][PF_6]_2$
formula	$C_{31}H_{36}F_{12}FeN_2O_2P_2$	$C_{64}H_{76}F_{24}Fe_2N_4O_4P_4$	$C_{45}H_{50}F_{12}Fe_2N_2O_3P_2$	$C_{37}H_{34}F_{12}Fe_2N_2P_2$
M	814.41	1656.87	1068.51	908.30
cryst syst	monoclinic	triclinic	monoclinic	orthorhombic
space group	$P2_1/c$	$P\bar{1}$	$C2/c$	$Aba2$
a/Å	19.543(2)	9.535(1)	30.310(4)	17.194(1)
b/Å	9.079(6)	13.158(1)	9.506(1)	20.923(2)
c/Å	20.569(2)	15.330(1)	17.093(1)	9.694(1)
α/deg	90	78.561(8)	90	90
β/deg	111.99(1)	72.432(9)	109.318(3)	90
γ/deg	90	73.010(8)	90	90
U/Å^3	3384.2(4)	1740.8(3)	4647.5(7)	3487.5(5)
Z	4	1	4	4
T/K	100(2)	100(2)	100(2)	100(2)
μ/mm^{-1}	0.640	0.623	0.784	1.021
cryst size/mm	0.30 × 0.12 × 0.04	0.20 × 0.08 × 0.04	0.30 × 0.18 × 0.10	0.15 × 0.08 × 0.02
cryst descript	dark green plate	dark green block	dark green lath	dark green lath
no. of reflns collected	11 633	5432	11 078	3033
no. of indep reflns (R_{int})	5974 (0.0585)	2726 (0.0802)	4031 (0.0574)	1168 (0.1240)
θ_{max}/deg (completeness)	25.03 (99.8%)	18.85 (99.6%)	25.04 (98.1%)	18.00 (99.4%)
reflections with $I > 2\sigma(I)$	3276	1400	2516	772
goodness-of-fit on F^2	0.816	1.270	1.080	0.910
final R_1, wR_2 $[I > 2\sigma(I)]$	0.0433, 0.0795	0.0507, 0.0898	0.0864, 0.1851	0.0542, 0.1149
(all data)	0.0901, 0.0862	0.1177, 0.1009	0.1367, 0.2097	0.0828, 0.1216
peak and hole/eÅ^{-3}	0.552, −0.364	0.374, −0.296	1.224, −0.672	0.392, −0.309

5.44−5.38 (2 H, m, CH_2), 4.84 (2 H, t, J = 1.9 Hz, C_5H_4), 4.75 (2 H, t, J = 1.9 Hz, C_5H_4), 4.26 (5 H, s, C_5H_5), 2.91 (3 H, s, Me). Anal. Calcd (%) for $C_{25}H_{24}F_{12}FeN_2P_2$: C, 43.00; H, 3.46; N, 4.01. Found: C, 42.70; H, 3.17; N, 3.84. MS: m/z = 552.9 ($[M - PF_6]^+$), 204.2 ($[M - 2PF_6]^{2+}$).

Synthesis of 2-Methyl-12-[(*E*)-2-(ferrocenyl)vinyl]-7,8-dihydro-6*H*-dipyrido[1,2-*a*:2′,1′-*c*]-[1,4]diazepinium Hexafluorophosphate, [4][PF$_6$]$_2$. This compound was prepared and purified in manner similar to $[3][PF_6]_2$ by using 1,3-bis(triflyloxy)propane (89 mg, 0.262 mmol) in place of 1,2-bis(triflyloxy)ethane, giving a dark green solid: 72 mg, 77%. ^{1}H NMR (400 MHz, $(CD_3)_2CO$): δ 9.27 (1 H, d, J = 6.6 Hz, C_5H_3N), 9.05 (1 H, d, J = 6.6 Hz, C_5H_3N), 8.58−8.54 (2 H, C_5H_3N), 8.39 (1 H, d, J = 6.6 Hz, C_5H_3N), 8.31 (1 H, d, J = 6.6 Hz, C_5H_3N), 8.18 (1 H, d, J = 15.9 Hz, CH), 7.15 (1 H, d, J = 15.9 Hz, CH), 5.29−5.21 (1 H, m, NCH_2^{eq}), 5.14−5.06 (1 H, m, NCH_2^{eq}), 4.95−4.81 (3 H, NCH_2^{ax} + C_5H_4), 4.75−4.60 (3 H, NCH_2^{ax} + C_5H_4), 4.25 (5 H, s, C_5H_5), 3.16−2.99 (2 H, m, CH_2), 2.87 (3 H, s, Me). Anal. Calcd (%) for $C_{26}H_{26}F_{12}FeN_2P_2\cdot 0.13Et_2O$: C, 44.12; H, 3.78; N, 3.88. Found: C, 44.42; H, 3.70; N, 3.74. MS: m/z = 567.2 ($[M - PF_6]^+$), 211.1 ($[M - 2PF_6]^{2+}$). The residual diethyl ether included in the isolated product is also evidenced by extra signals with the appropriate integrals in the ^{1}H NMR spectrum (quartet at 3.45 ppm and triplet at 1.15 ppm).

Synthesis of 2,11-Bis[(*E*)-2-(ferrocenyl)vinyl]-6,7-dihydrodipyrido[1,2-*a*:2′,1′-*c*]pyrazinediium Hexafluorophosphate, [5][PF$_6$]$_2$. This compound was prepared and purified in manner similar to $[3][PF_6]_2$ by using 1,2-bis(triflyloxy)ethane (57 mg, 0.175 mmol) in dry DCM (ca. 0.6 mL) and $2\cdot 0.33H_2O$ (50 mg, 85.9 μmol) in chloroform (20 mL). A dark green solid was obtained: 38 mg, 48%. ^{1}H NMR (400 MHz, $(CD_3)_2CO$): δ 9.09 (2 H, d, J = 6.6 Hz, C_5H_3N), 9.01 (2 H, d, J = 1.8 Hz, C_5H_3N), 8.39 (2 H, d, J = 6.6 Hz, C_5H_3N), 8.27 (2 H, d, J = 15.9 Hz, 2CH), 7.20 (2 H, d, J = 15.9 Hz, 2CH), 5.41 (4 H, s, $2CH_2$), 4.87 (4 H, t, J = 1.8 Hz, $2C_5H_4$), 4.76 (4 H, t, J = 1.8 Hz, $2C_5H_4$), 4.29 (10 H, s, $2C_5H_5$). Anal. Calcd (%) for $C_{36}H_{32}F_{12}Fe_2N_2P_2\cdot 0.33Et_2O$: C, 48.79; H, 3.80; N, 3.05. Found: C, 48.95; H, 3.66; N, 3.21. MS: m/z = 749.9 ($[M - PF_6]^+$), 302.2 ($[M - 2PF_6]^{2+}$). The residual diethyl ether included in the isolated product is also evidenced by extra signals with the appropriate integrals in the ^{1}H NMR spectrum (see above).

Synthesis of 2,12-Bis[(*E*)-2-(ferrocenyl)vinyl]-7,8-dihydro-6*H*-dipyrido[1,2-*a*:2′,1′-*c*]-[1,4]diazepinium Hexafluorophosphate, [6][PF$_6$]$_2$. This compound was prepared in manner similar to $[5][PF_6]_2$ by using 1,3-bis(triflyloxy)propane (30 mg, 0.088 mmol) in place of 1,2-bis(triflyloxy)ethane in dry DCM (ca. 0.3 mL) and $2\cdot 0.33H_2O$ (25 mg, 0.043 mmol). The crude $[6][OTf]_2$ was dissolved in a minimum amount of 1:1 ethanol/acetone, metathesized to its PF_6^- salt, and reprecipitated as for $[5][PF_6]_2$ to yield a dark green solid: 22 mg, 56%. ^{1}H NMR (400 MHz, $(CD_3)_2CO$): δ 9.09 (2 H, d, J = 6.6 Hz, C_5H_3N), 8.64 (2 H, d, J = 2.3 Hz, C_5H_3N), 8.37 (2 H, d, J = 6.6 Hz, C_5H_3N), 8.23 (2 H, d, J = 15.9 Hz, 2CH), 7.20 (2 H, d, J = 15.9 Hz, 2CH), 5.17−5.09 (2 H, m, NCH_2^{eq}), 4.89−4.86 (2 H, m, C_5H_4), 4.84−4.82 (2 H, m, C_5H_4), 4.80−4.74 (2 H, m, NCH_2^{ax}), 4.74−4.70 (4 H, m, $2C_5H_4$), 4.27 (10 H, s, $2C_5H_5$), 3.09−3.01 (2 H, m, CH_2). Anal. Calcd (%) for $C_{37}H_{34}F_{12}Fe_2N_2P_2$: C, 48.93; H, 3.77; N, 3.08. Found: C, 48.67; H, 3.68; N, 3.10. MS: m/z = 763.3 ($[M - PF_6]^+$), 309.2 ($[M - 2PF_6]^{2+}$).

X-ray Crystallography. Crystals were obtained by diffusion of diethyl ether vapor into acetone solutions at room temperature. Data were collected on an Oxford Diffraction XCalibur 2 X-ray diffractometer by using Mo Kα radiation (λ = 0.71073 Å). The data were processed by using the Oxford Diffraction CrysAlis RED[22] software package, and the structures solved by direct methods by using SIR-97[23a] or SIR-2004[23b] *via* WinGX[24] or SHELXS-97.[25] Refinement was achieved by full-matrix least-squares on all F_o^2 data using SHELXL-97.[26] With the exception of $[6][PF_6]_2$, all non-hydrogen atoms were refined anisotropically, and

dx.doi.org/10.1021/om200604f |*Organometallics* 2011, 30, 5731–5743

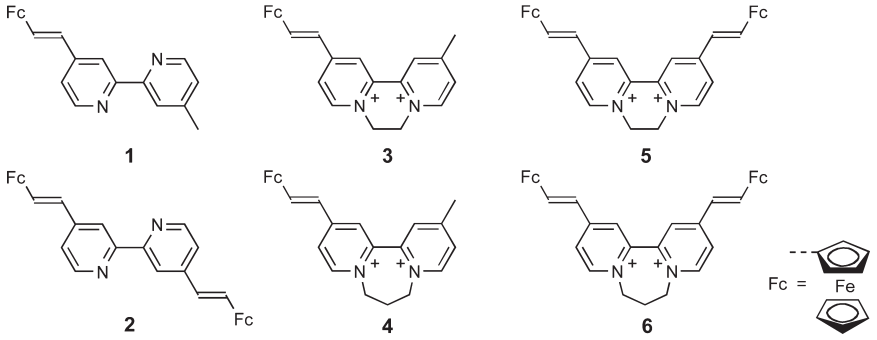

Figure 1. Chemical structures of the Fc DQ^{2+} chromophores and their precursors. Abbreviations: EDQ^{2+} = ethylene diquat; PDQ^{2+} = propylene diquat. All of the measurements were made by using PF_6^- salts.

hydrogen atoms were included in idealized positions by using the riding model, with thermal parameters of 1.2 times those of aromatic parent carbon atoms and 1.5 times those of methyl parent carbons. For [**6**]-$[PF_6]_2$ the quantity of data was very low, so only Fe, P, and F atoms were refined anisotropically: multiple attempts were made to grow crystals, but the data set presented is the best that could be obtained. All other calculations were carried out by using the SHELXTL package.[27] Crystallographic data and refinement details are presented in Table 1. The asymmetric units have the following compositions: for $[\mathbf{3}][PF_6]_2 \cdot 2Me_2CO$, one dication, both acetone molecules, and two PF_6^- anions shared between three crystallographically independent positions (occupancies 1, 0.5, 0.5); for $[\mathbf{4b}][PF_6]_4 \cdot 4Me_2CO$, half a $[\mathbf{4b}]^{4+}$ cation, two PF_6^- anions, and two acetone molecules; for $[\mathbf{5}][PF_6]_2 \cdot 3Me_2CO$, half a dication, one disordered PF_6^- anion, and one disordered and one 50% occupied acetone molecule; for $[\mathbf{6}][PF_6]_2$ half a dication and one PF_6^- anion.

Hyper-Rayleigh Scattering. Details of the hyper-Rayleigh scattering (HRS) experiment have been discussed elsewhere,[28] and the experimental procedure used was as previously described.[29] β values were determined by using the electric-field-induced second-harmonic-generation β_{1064} for *p*-nitroaniline (25.9×10^{-30} esu in acetone)[30] as an external reference. All measurements were performed by using the 1064 nm fundamental of an injection-seeded, Q-switched Nd:YAG laser (Quanta-Ray GCR-5, 8 ns pulses, 7 mJ, 10 Hz). Dilute acetone solutions (10^{-5}–10^{-6} M) were used to ensure a linear dependence of $I_{2\omega}/I_\omega^2$ on solute concentration, precluding the need for Lambert–Beer correction factors. Samples were filtered (Millipore, 0.45 μm), and none showed any fluorescence. HRS depolarization ratios ρ[31] were determined at 1064 nm according to a published methodology.[32] The parameter ρ is the ratio of the intensities of the scattered SH light polarized parallel and perpendicular to the vertical polarization direction of the fundamental beam.

Stark Spectroscopy. The Stark apparatus, experimental methods, and data collection procedure were as previously reported,[33] except that a Xe arc lamp was used as the light source in place of a W filament bulb. Butyronitrile was used as the glassing medium, for which the local field correction f_{int} is estimated as 1.33,[33] and the Stark spectrum for each compound was measured at least twice. Satisfactory fits of the Stark data for the salts $[\mathbf{3}][PF_6]_2$ and $[\mathbf{4}][PF_6]_2$ were obtained by using the observed absorption spectra, but for $[\mathbf{5}][PF_6]_2$ and $[\mathbf{6}][PF_6]_2$ these spectra were modeled with a sum of three Gaussian curves that reproduce the data and separate the peaks. The first and second derivatives of the Gaussian curves were then used to fit the Stark spectra with Liptay's equation.[34] The dipole-moment change $\Delta\mu_{12} = \mu_e - \mu_g$ (where μ_e and μ_g are the respective excited- and ground-state dipole moments, associated with each of the optical transitions considered in the fit) was then calculated from the coefficient of the second-derivative component. While the Gaussian fitting functions may not necessarily have physical meaning in themselves (in terms of accurately representing individual electronic transitions), they are essential in order to allow the derivation of Stark data. Note that analyses of the combined data for the complete ICT bands are shown here and in other studies[5h,19b,19c,35] to afford physically sensible results and trends.

A two-state analysis of the ICT transitions gives

$$\Delta\mu_{ab}^2 = \Delta\mu_{12}^2 + 4\mu_{12}^2 \quad (1)$$

where $\Delta\mu_{ab}$ is the dipole-moment change between the diabatic states and $\Delta\mu_{12}$ is the observed (adiabatic) dipole-moment change. The value of μ_{12} can be determined from the oscillator strength f_{os} of the transition by

$$|\mu_{12}| = \left(\frac{f_{os}}{1.08 \times 10^{-5} E_{max}}\right)^{1/2} \quad (2)$$

where E_{max} is the energy of the ICT maximum (in wavenumbers) and μ_{12} is in eÅ. The latter is converted into Debye units upon multiplying by 4.803. The degree of delocalization c_b^2 and electronic coupling matrix element H_{ab} for the diabatic states are given by

$$c_b^2 = \frac{1}{2}\left[1 - \left(\frac{\Delta\mu_{12}^2}{\Delta\mu_{12}^2 + 4\mu_{12}^2}\right)^{1/2}\right] \quad (3)$$

$$|H_{ab}| = \left|\frac{E_{max}(\mu_{12})}{\Delta\mu_{ab}}\right| \quad (4)$$

If the hyperpolarizability tensor β_0 has only nonzero elements along the CT direction, then this quantity is given by

$$\beta_0 = \frac{3\Delta\mu_{12}(\mu_{12})^2}{(E_{max})^2} \quad (5)$$

A relative error of ±20% is estimated for the β_0 values derived from the Stark data and using eq 5, while experimental errors of ±10% are estimated for μ_{12}, $\Delta\mu_{12}$, and $\Delta\mu_{ab}$, ±15% for H_{ab}, and ±50% for c_b^2. Note that the ±20% uncertainty for the β_0 values is merely statistical and does not account for any errors introduced by two-state extrapolation.

RESULTS AND DISCUSSION

Syntheses and Characterization. The structures of 2,2′-bipyridyl precursors **1** and **2** and their diquaternized derivatives **3**–**6** are shown in Figure 1. Compounds **1** and **2** are obtained by reacting 4-[(diethoxyphosphinyl)methyl]-4′-methyl-2,2′-bipyridyl or 4,4′-bis[(diethoxyphosphinyl)methyl]-2,2′-bipyridyl, respectively, with ferrocenecarboxaldehyde and potassium *tert*-butoxide in THF. This Wadsworth–Emmons-type approach

dx.doi.org/10.1021/om200604f |*Organometallics* 2011, 30, 5731–5743

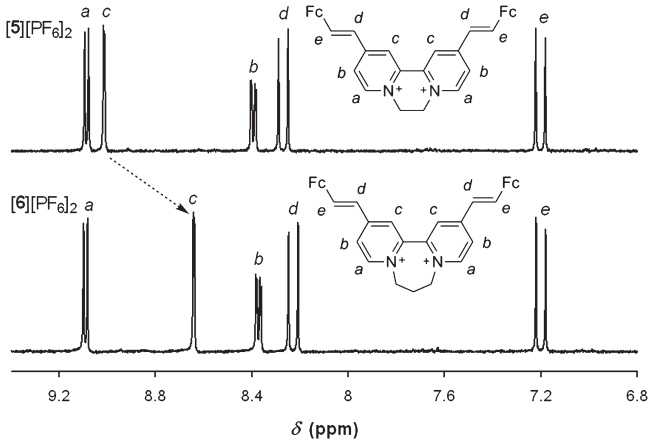

Figure 2. Aromatic regions of the ^{1}H NMR spectra of the salts $[\mathbf{5}][PF_6]_2$ and $[\mathbf{6}][PF_6]_2$ recorded at 400 MHz in $(CD_3)_2CO$ at 293 K. The arrow indicates the largest shift observed for one of the C_5H_3N signals.

produces the desired precursors in high yields (ca. 80%) with minimal need for purification. **1** and **2** have been prepared previously by treating 4,4′-dimethyl-2,2′-bipyridyl with lithium diisopropylamide, followed by reaction with ferrocenecarboxaldehyde and subsequent dehydration in the presence of pyridinium 4-toluenesulfonate.[36]

To effect diquaternization, **1** and **2** are treated with two equivalents of 1,2-bis(triflyloxy)ethane or 1,3-bis(triflyloxy)propane at room temperature, following our own precedent.[37] While reactions of **1** to produce the monosubstituted (MS) chromophores **3** and **4** proceed effectively in DCM, the poor solubility of the disubstituted (DS) precursor **2** in this solvent necessitates the use of chloroform for the syntheses of **5** and **6**. The chromophores are purified via anion metathesis to their PF_6^- salts, followed by reprecipitation from acetone with diethyl ether. The dark green solids are isolated in yields in the range ca. 50−75%. All of the new compounds give clean ^{1}H NMR spectra (see below) and satisfactory CHN elemental analyses and +electrospray mass spectra.

^{1}H NMR Spectroscopy. The complex salts $[\mathbf{3}-\mathbf{6}][PF_6]_2$ give diagnostic ^{1}H NMR spectra, the MS and DS chromophores being readily distinguished by the relative intensities of the Fc signals, the presence or absence of a methyl signal, and the number of signals for the C_5H_3N rings. The DS species give only three C_5H_3N signals, while the less symmetric MS compounds give six, of which some are overlapped. As well as showing different numbers of ^{1}H NMR signals for their CH_2 protons, the aromatic regions for the EDQ^{2+} chromophores **3** and **5** differ significantly from those of their PDQ^{2+} analogues **4** and **6**. Representative spectra for the DS compounds $[\mathbf{5}][PF_6]_2$ and $[\mathbf{6}][PF_6]_2$ are shown in Figure 2. The finely split doublet signal associated with the protons located adjacent to the bridge between the two pyridyl rings (H^c) shifts from δ = 9.01 pm in $[\mathbf{5}][PF_6]_2$ to δ = 8.64 ppm in $[\mathbf{6}][PF_6]_2$. These signals show similar differences in purely organic DQ^{2+} derivatives,[19b,c] attributable to weaker deshielding in the more twisted and less strongly electron-withdrawing PDQ^{2+} units.

The ^{1}H NMR spectra of $[\mathbf{3}-\mathbf{6}][PF_6]_2$ also show evidence for rotamers. The PDQ^{2+} derivatives $[\mathbf{4}/\mathbf{6}][PF_6]_2$ in $(CD_3)_2CO$ at 293 K show three, rather than the expected two, C_5H_4 signals, since the downfield one splits into two at δ = 4.84 and 4.81 ppm for $[\mathbf{4}][PF_6]_2$ and δ = 4.89−4.86 and 4.84−4.82 ppm for $[\mathbf{6}][PF_6]_2$. On warming a $(CD_3)_2CO$ solution of $[\mathbf{4}][PF_6]_2$ to 313 K, these two downfield signals begin to merge. Although not observed in CD_3CN at 293 K, splitting of the downfield C_5H_4 signal is also observed in the spectra of $[\mathbf{4}/\mathbf{6}][PF_6]_2$ in CD_3CN at 233 K (Figure 3a). These observations are consistent with sterically restricted rotation around a $C-C_5H_4$ bond.[38] The solvent dependence (to our knowledge unreported in Fc species) suggests that the rotational barrier is low and that the bulkier, less polar acetone is more able than acetonitrile to impede molecular motions and/or less able to screen attractive interactions between the Fe^{II} center and the cationic π-system. Such interactions are known to cause restricted rotation in Fc organocations.[38b,g]

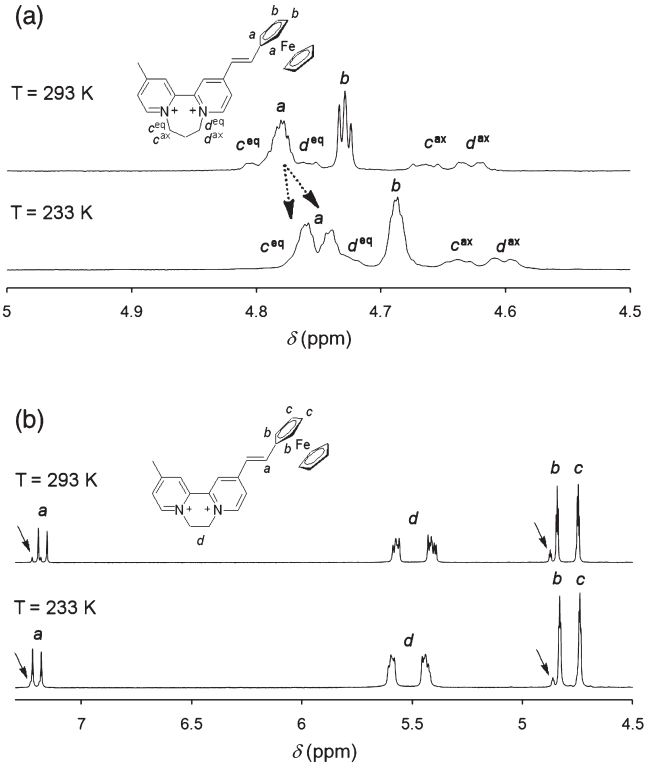

Figure 3. Variable-temperature ^{1}H NMR spectra showing evidence for rotamers in (a) $[\mathbf{4}][PF_6]_2$ in CD_3CN (arrows indicate the splitting of the downfield C_5H_4 protons into two signals); (b) $[\mathbf{3}][PF_6]_2$ in $(CD_3)_2CO$ (arrows indicate minor vinyl and C_5H_4 signals).

In addition, well-resolved spectra of the MS compounds $[\mathbf{3}/\mathbf{4}][PF_6]_2$ in both $(CD_3)_2CO$ and CD_3CN reveal small secondary vinyl CH doublets, Fc signals, and DQ^{2+} signals. These integrate to ca. 20% of the total for the chemical environments concerned. Comparison of the total integrals with those for other proton environments indicates that the extra signals do not result from impurities, and coupling constants of ca. 15 Hz show that the *E*-stereochemistry of the double bonds is retained. These observations suggest slow exchange between favored and disfavored rotational conformers. Upon cooling $[\mathbf{3}][PF_6]_2$ to 233 K in $(CD_3)_2CO$, some of the minor signals recombine with the major signals and others become slightly weaker as the disfavored conformation becomes less accessible (Figure 3b). Substantial broadening of the signals (from ca. 0.015 to 0.03−0.05 ppm) seems to prevent observation of these minor resonances in the DS compounds.

dx.doi.org/10.1021/om200604f |*Organometallics* 2011, 30, 5731–5743

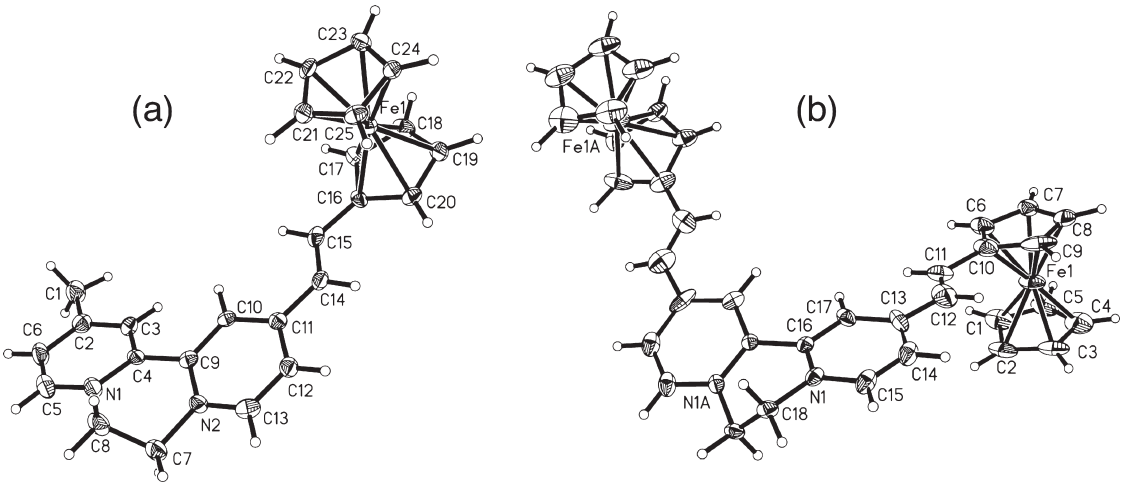

Figure 4. Representations of the molecular structures of the complex cations in (a) $[3][PF_6]_2 \cdot 2Me_2CO$ (50% probability ellipsoids) and (b) $[5][PF_6]_2 \cdot 3Me_2CO$ (30% probability ellipsoids). Anions, solvent molecules, and disorder (in b) are omitted for clarity.

X-ray Crystallography. We have obtained single-crystal X-ray structures for the salts $[3][PF_6]_2 \cdot 2Me_2CO$, $[5][PF_6]_2 \cdot 3Me_2CO$, and $[6][PF_6]_2$; representations of the complex cations are shown in Figures 4 and 5. Additional structures of $[5][PF_6]_2 \cdot 3MeCN$ and $[6][PF_6][OTf]$ are included in the Supporting Information.

The salt $[3][PF_6]_2 \cdot 2Me_2CO$ gives the highest quality reproducible structure obtained in this study (Figure 4a), with unremarkable bond distances and angles (Supporting Information, Table S1). The dihedral angle between the pyridyl rings of the EDQ^{2+} unit (py/py, ca. 19.3°) is within the range for published structures (15−24°),[39] and there is a slight twist of ca. 3.4° between the C_5H_4 and vinyl-linked pyridyl rings (C_5H_4/py). The geometric parameters of $[5][PF_6]_2 \cdot 3Me_2CO$ (Figure 4b) are largely comparable to those in its MS counterpart, but the vinyl distance (C11−C12) is considerably shorter (1.227(11), cf. 1.336(4) Å in $[3][PF_6]_2 \cdot 2Me_2CO$), and disorder in the Fc moiety gives a greater range (and lower precision) of Fe−C bond distances (1.87(4)−2.14(3) Å). Note that in the structure of $[5][PF_6]_2 \cdot 3MeCN$ (Supporting Information, Figure S1 and Table S2), which is poorer quality overall than that of $[5][PF_6]_2 \cdot 3Me_2CO$ but lacks disorder, the vinyl distances are much closer to those in $[3][PF_6]_2 \cdot 2Me_2CO$. In $[5][PF_6]_2 \cdot 3Me_2CO$, the py/py and C_5H_4/py dihedral angles are ca. 24.7° and 8.3°, respectively, both larger than in $[3][PF_6]_2 \cdot 2Me_2CO$. The extended structures are centrosymmetric due to antiparallel alignment of adjacent layers of cations in $[3][PF_6]_2 \cdot 2Me_2CO$ and chains of cations in $[5][PF_6]_2 \cdot 3Me_2CO$.

The salt $[6][PF_6]_2$ crystallizes in the noncentrosymmetric space group *Aba*2. A perfectly polar packing of the chromophore dipoles (Figure 5) means that this material is expected to show bulk quadratic NLO behavior, as also found for a 4-(dimethylamino)-phenyl-substituted PDQ^{2+} derivative.[19b] Furthermore, the relatively high symmetry structure of $[6][PF_6]_2$ (orthorhombic) should facilitate crystal growth, including the production of single-crystalline thin films for potential applications in integrated optics.[40] The absence of any included solvent in this particular material is an additional feature that improves its prospects for device purposes. The molecular structure of $[6]^{2+}$ is generally similar to that of $[5]^{2+}$, except for a much larger py/py dihedral angle (ca. 54.2°) due to the extended diquaternizing bridge; this is in the range found in other PDQ^{2+} structures.[19b,c]

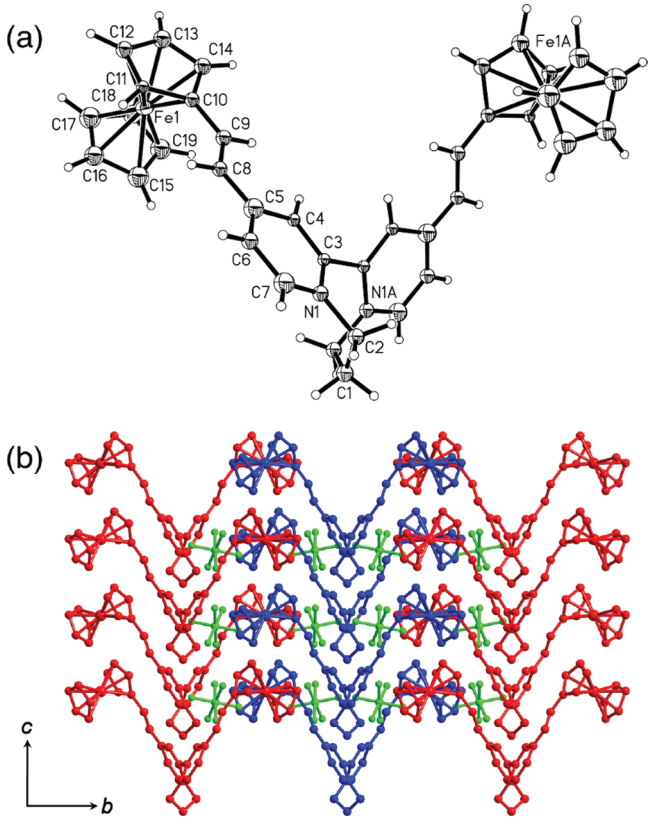

Figure 5. (a) Representation of the molecular structure of the cation in $[6][PF_6]_2$ (50% probability ellipsoids). (b) Packing in $[6][PF_6]_2$ viewed along the crystallographic *a* axis. Alternate rows of dications are red and blue, PF_6^- anions are green, and H atoms are omitted.

The C_5H_4/py dihedral angle in $[6][PF_6]_2$ (ca. 17.0°) is also larger than that in $[5][PF_6]_2 \cdot 3Me_2CO$.

Attempted crystallization of $[4][PF_6]_2$ from acetone/diethyl ether led to a low-resolution (1.1 Å) structure showing that the $[4]^{2+}$ cations unexpectedly dimerize, producing $[\mathbf{4b}]^{4+}$ (Figure 6) in low yield. This process involves a Michael reaction between the methyl and vinyl groups. In the novel macrocycle, two PDQ^{2+}

units are connected by two saturated, Fc-substituted C_3 linkers (C−C distances 1.60(1) and 1.51(1) Å). The overall centrosymmetric solid-state structure of $[\mathbf{4b}][PF_6]_4\cdot 4Me_2CO$ is based on a diastereomeric $[\mathbf{4b}]^{4+}$ cation, with opposing helical twists of the two PDQ^{2+} units, as seen in the N(1)−C(14)−C(5)−N(2) (clockwise) and N(1A)−C(14A)−C(5A)−N(2A) (anticlockwise) torsions. Further details concerning this material can be found in the Supporting Information. The +ESI mass spectrum shows a peak at m/z = 567 with an isotope pattern perfectly matching $([\mathbf{4b}][PF_6]_2)^{2+}$ (Figure S3), while the ^{1}H NMR spectrum indicates a symmetric DQ^{2+} environment without methyl or vinyl protons. The CH_2 protons on C(1)/C(1A) and C(15)/C(15A) are diastereotopic, and the ^{1}H NMR spectrum (at 293 K in $(CD_3)_2CO$) shows two complex 4H multiplets characteristic of diastereotopic protons, rather than the simple 8H doublet expected for four chemically and magnetically equivalent CH_2 groups. In addition, the UV−vis spectrum (Figure S4) lacks an intense, low-energy MLCT band characteristic of the conjugated chromophores **1**−**4**. Unlike recently reported nonracemic diquats containing eight-membered rings,[41] $[\mathbf{4b}]^{4+}$ appears to be conformationally flexible at room temperature.

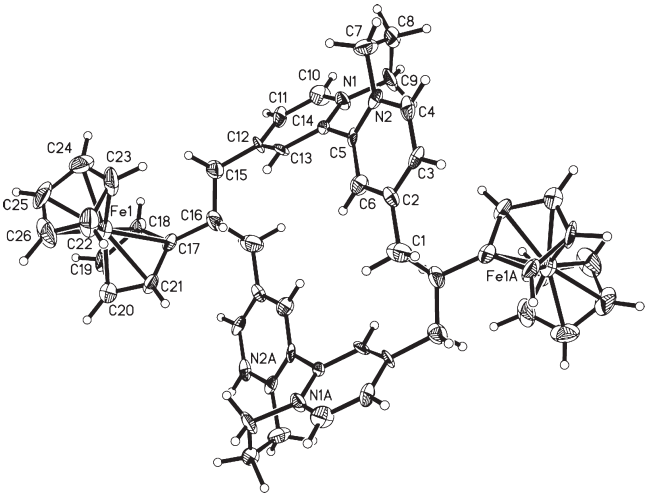

Figure 6. Representation of the molecular structure of the cation in $[\mathbf{4b}][PF_6]_4\cdot 4Me_2CO$, with the anions and solvent molecules omitted for clarity (50% probability ellipsoids).

Electronic Spectroscopy. The UV−vis absorption spectra of the complex salts $[\mathbf{3}-\mathbf{6}][PF_6]_2$ have been recorded in acetonitrile; the results are summarized in Table 2 and also depicted in Figure 7. Although the compounds do show some degree of instability in acetonitrile, this solvent was used because it provides the widest spectroscopic window.

Each compound shows a broad, visible band with λ_{max} in the range ca. 610−660 nm and two bands in the UV region with λ_{max} values in the ranges ca. 390−410 and 290−310 nm. According to previous studies,[18] the low-energy bands are assigned as MLCT in character, while the UV bands are due to $\pi \rightarrow \pi^*$ transitions, with the most intense one having significant ILCT character. For comparison, the neutral precursor compounds **1** and **2** both show MLCT bands at λ_{max} = 470 nm in acetonitrile, together with three UV bands (λ_{max} = 376, 310/316 and 252/255 nm).[36] Diquaternization hence causes marked spectral changes, with the MLCT energy decreasing by as much as ca. 0.8 eV due to the dramatic enhancement of the electron-accepting ability of the 2,2′-bipyridyl unit.

All three absorptions of $[\mathbf{3}-\mathbf{6}][PF_6]_2$ show blue shifts on changing from an EDQ^{2+} derivative to its PDQ^{2+} counterpart

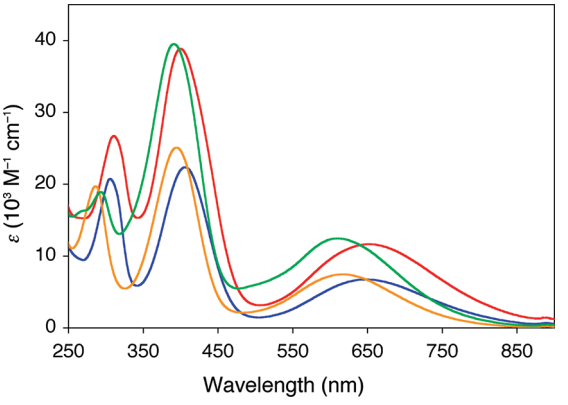

Figure 7. UV−vis absorption spectra of $[\mathbf{3}][PF_6]_2$ (blue), $[\mathbf{4}][PF_6]_2$ (gold), $[\mathbf{5}][PF_6]_2$ (red), and $[\mathbf{6}][PF_6]_2$ (green) at 293 K in acetonitrile.

Table 2. UV−Vis Absorption and Electrochemical Data for Salts $[\mathbf{3}-\mathbf{6}][PF_6]_2$ in Acetonitrile[a]

				E, V vs Ag−AgCl (ΔE_p, mV)[b]	
dication	λ_{max}, nm[a] (ε, 10^3 M^{-1} cm^{-1})	E_{max} (eV)	assignment	$E_{1/2}[Fe^{III/II}]$	$E_{1/2}$, reductions
3	648 (6.75)	1.91	MLCT	0.63 (90)	−0.42 (85)
	406 (22.4)	3.05	ILCT		−0.83 (90)
	306 (20.7)	4.05	$\pi \rightarrow \pi^*$		
4	617 (7.45)	2.01	MLCT	0.63 (80)	−0.58 (80)
	395 (25.1)	3.14	ILCT		−0.89 (90)
	286 (19.7)	4.34	$\pi \rightarrow \pi^*$		
5	658 (11.6)	1.88	MLCT	0.64 (95)	−0.38 (90)
	400 (38.9)	3.10	ILCT		−0.76 (85)
	311 (26.7)	3.99	$\pi \rightarrow \pi^*$		
6	610 (12.5)	2.03	MLCT	0.63 (85)	−0.56 (70)
	391 (39.5)	3.17	ILCT		−0.82 (75)
	293 (18.9)	4.23	$\pi \rightarrow \pi^*$		

[a] Solutions ca. (2−3) × 10^{-5} M. [b] Solutions ca. 10^{-3} M in analyte and 0.1 M in $[NBu^n_4]PF_6$ at a 2 mm disk glassy carbon working electrode with a scan rate of 200 mV s^{-1}. Ferrocene internal reference $E_{1/2}$ = 0.46 V, ΔE_p = 70−90 mV.

dx.doi.org/10.1021/om200604f |*Organometallics* 2011, 30, 5731–5743

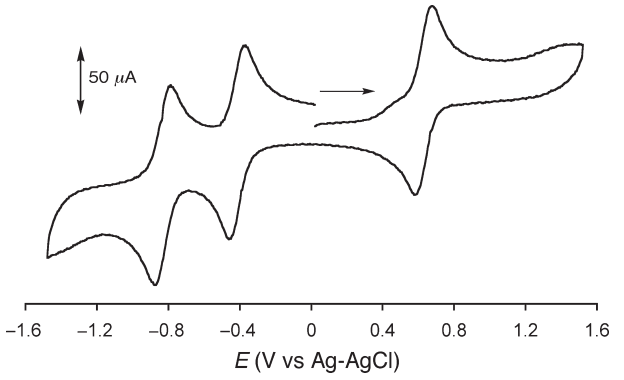

Figure 8. Cyclic voltammograms for the salt $[\mathbf{3}][PF_6]_2$ recorded at 200 mV s^{-1} in acetonitrile with a glassy carbon working electrode. The arrow indicates the direction of the initial scan.

(Figure 7). The MLCT and ILCT band energies increase by 0.07−0.15 eV, while E_{max} for the highest energy band is more strongly affected, increasing by 0.29 eV (**3** → **4**) or 0.24 eV (**5** → **6**). These blue shifts are consistent with the weaker accepting strength of PDQ^{2+} when compared with EDQ^{2+} and reflect the behavior of purely organic DQ^{2+} derivatives.[19b,c] The molar extinction coefficients (ε) are not greatly affected by this structural change. Upon changing from a MS to the related DS chromophore, the intensities of the MLCT and ILCT bands increase substantially, while the highest energy band shows inconsistent behavior. The band energies show small accompanying changes, but no clear trend.

Acetone was chosen as the solvent for HRS measurements (see below) because the new chromophores show higher stability in this medium than in acetonitrile. As shown in the Supporting Information (Figure S5 and Table S3), the absorption spectra are largely independent of the solvent, but the $\pi \rightarrow \pi^*$ bands at ca. 300 nm are obscured by the narrower solvent window of acetone.

Electrochemistry. We have investigated salts $[\mathbf{3}-\mathbf{6}][PF_6]_2$ by using cyclic voltammetry in acetonitrile, and the results are presented in Table 2. A representative cyclic voltammogram of $[\mathbf{3}][PF_6]_2$ is shown in Figure 8.

Each compound shows a reversible $Fe^{III/II}$ oxidation process with $E_{1/2}$ = ca. 0.63 V vs Ag−AgCl and two reversible waves associated with reductions of the DQ^{2+} units with $E_{1/2}$ in the range −0.38 to −0.89 V vs Ag−AgCl (Table 2). These $Fe^{III/II}$ waves are shifted anodically by ca. 80 mV when compared with the precursors **1** and **2**,[36] due to the increased electron-withdrawing influence of the 2,2′-bipyridyl unit on diquaternization. The presence of three, well-resolved redox couples means that these Fc diquats have a total of four accessible oxidation states; these can be expected to possess strongly variable optical absorption and NLO properties. While $E_{1/2}[Fe^{III/II}]$ is essentially constant for all four complexes, the peak currents are larger for the DS compounds when compared with their MS analogues because the waves correspond with two-electron processes in the former. The observation of only one $Fe^{III/II}$ wave for the DS species shows that the two Fc units are not significantly coupled electronically. As observed in purely organic DQ^{2+} derivatives,[19b,c] the two reduction processes are cathodically shifted on moving from an EDQ^{2+} derivative to its PDQ^{2+} analogue. The first wave shifts by 160−180 mV, while smaller shifts of −60 mV are observed for the second one. These changes arise from the weaker electron-accepting ability of PDQ^{2+} with respect to EDQ^{2+} (see above). Changing from a MS compound to its DS counterpart causes the potentials for the reductive processes to increase by 20−40 mV (first wave) and 70 mV (second wave); the increased size of the π-systems allows more effective delocalization of the additional charge(s) and therefore facilitates reduction.

Hyper-Rayleigh Scattering. The β values of salts $[\mathbf{3}-\mathbf{6}][PF_6]_2$ were measured in acetone solutions by using the HRS technique[28,29] with a 1064 nm Nd^{3+}:YAG laser, and the results are shown in Table 3. The hyperpolarizability data shown are orientationally averaged $(\langle\beta^2_{HRS}\rangle)^{1/2}$ values derived from the total HRS intensity, regardless of molecular symmetry. Due to the proximity of the absorption band(s) to the second-harmonic wavelength (532 nm), all of the β values are enhanced by resonance.

Comparing the $(\langle\beta^2_{HRS}\rangle)^{1/2}$ values for the EDQ^{2+} derivatives **3** and **5** shows a significant increase on moving from the MS chromophore to its DS counterpart. However, the values for the PDQ^{2+} species **4** and **6** are not significantly different. In addition, no clear trend relating to the EDQ^{2+} vs PDQ^{2+} comparison is evident.

Due to their nonlinear molecular shapes, the β responses of **3**−**6** are expected to possess 2D character. Therefore, we have also measured HRS depolarization ratios ρ, and these are included in Table 3. As expected, the ρ values are generally somewhat lower than that of 3.5 obtained for the dipolar reference compound 4-nitroaniline. A C_{2v} symmetric molecule under Kleinman symmetry has only two significant components of the β tensor, β_{zzz} and β_{zyy}, which can be determined from averaged $\langle\beta^2_{HRS}\rangle$ and ρ as follows:

$$\begin{cases} \langle\beta^2_{HRS}\rangle = \langle\beta^2_{ZZZ}\rangle + \langle\beta^2_{YZZ}\rangle \\ \rho = \dfrac{\langle\beta^2_{ZZZ}\rangle}{\langle\beta^2_{YZZ}\rangle} \end{cases} \quad (6)$$

The HRS intensities with parallel polarization for fundamental and SH wavelengths, $\langle\beta^2_{ZZZ}\rangle$, and for perpendicular polarization, $\langle\beta^2_{YZZ}\rangle$, are given in terms of the molecular tensor components β_{zzz} and β_{zyy} according to

$$\begin{cases} \langle\beta^2_{ZZZ}\rangle = \dfrac{1}{7}\beta^2_{zzz} + \dfrac{6}{35}\beta_{zzz}\beta_{zyy} + \dfrac{9}{35}\beta^2_{zyy} \\ \langle\beta^2_{YZZ}\rangle = \dfrac{1}{35}\beta^2_{zzz} - \dfrac{2}{105}\beta_{zzz}\beta_{zyy} + \dfrac{11}{105}\beta^2_{zyy} \end{cases} \quad (7)$$

and ρ can be expressed in terms of the parameter $k = \beta_{zyy}/\beta_{zzz}$ by

$$\rho = \frac{15 + 18k + 27k^2}{3 - 2k + 11k^2} \quad (8)$$

The values of β_{zzz} and β_{zyy} derived by using eqs 6−8 are shown in Table 3. In all cases, β_{zyy} is dominant. However, it is worth noting that the results of ρ measurements can be misleading, due to resonance effects and Kleinman symmetry breaking.[8g,42] Therefore, the quoted values of β_{zzz} and β_{zyy} for our new Fc chromophores may be questionable, but the 2D nature of their β responses is clear.

Stark Spectroscopy. The salts $[\mathbf{3}-\mathbf{6}][PF_6]_2$ have been studied by using Stark spectroscopy in butyronitrile glasses at 77 K, and the results are presented in Table 4. For the MS compounds, the observed data were fitted directly, but Gaussian fitting of the absorption spectra with three curves for each of the MLCT and ILCT bands was necessary to successfully model the Stark data for the DS compounds. Representative MLCT absorption and electroabsorption spectra for the salts $[\mathbf{3}][PF_6]_2$,

Table 3. HRS Data and Depolarization Ratios for Salts $[3-6][PF_6]_2$ in Acetone

dication	$(\langle\beta^2_{HRS}\rangle)^{1/2}$,[a] ($10^{-30}$ esu)	ρ[b]	k	β_{zzz},[c] (10^{-30} esu)	β_{zyy},[c] (10^{-30} esu)
3	80 ± 10	2.1 ± 0.4	>10	13 ± 2	130 ± 20
4	100 ± 15	2.5 ± 0.3	10	16 ± 3	160 ± 30
5	160 ± 35	2.1 ± 0.4	>10	26 ± 8	260 ± 75
6	90 ± 55	2.8 ± 0.8	3.3	42 ± 26	140 ± 80

[a] Total molecular HRS response without any assumption of symmetry or contributing tensor elements, measured in acetone by using a 1064 nm Nd^{3+}:YAG laser. The quoted cgs units (esu) can be converted into SI units ($C^3\ m^3\ J^{-2}$) by dividing by a factor of 2.693×10^{20}. [b] Depolarization ratio. [c] Hyperpolarizability tensor components derived from the HRS intensity and depolarization ratio measurements by using eqs 6−8.

Table 4. ICT Absorption and Stark Spectroscopic Data for Salts $[3-6][PF_6]_2$

dication	ν_{max}[a] (cm^{-1})	λ_{max}[a] (nm)	E_{max}[a] (eV)	f_{os}[b]	μ_{12}[c] (D)	$\Delta\mu_{12}$[d] (D)	$\Delta\mu_{ab}$[e] (D)	r_{12}[f] (Å)	r_{ab}[g] (Å)	c_b^2[h]	H_{ab}[i] ($10^3\ cm^{-1}$)	β_0[j] (10^{-30} esu)	$\Sigma\beta_0$ (10^{-30} esu)
3	15970	626	1.98	0.12	3.9	17.5	19.1	3.6	4.0	0.05	3.2	77	131
	25003	400	3.10	0.35	5.5	15.0	18.6	3.1	3.9	0.10	7.3	54	
4	16776	596	2.08	0.12	4.0	15.6	17.5	3.2	3.6	0.06	3.8	65	121
	25810	387	3.20	0.44	6.0	12.9	17.6	2.7	3.7	0.14	8.8	56	
5	14640 (15808)	687 (633)	1.82 (1.96)	0.04	2.3	21.2	21.7	4.4	4.5	0.01	1.6	41 (122)	206
	15994	628	1.98	0.09	3.5	16.8	18.3	3.5	3.8	0.04	3.1	62	
	17391	575	2.16	0.04	2.1	18.6	19.0	3.9	4.0	0.01	1.9	19	
	23138 (25164)	432 (397)	2.87 (3.12)	0.04	2.0	16.1	16.6	3.4	3.5	0.01	2.8	9 (84)	
	24305	411	3.01	0.14	3.5	17.3	18.7	3.6	3.9	0.04	4.6	28	
	25764	388	3.19	0.30	5.0	16.3	19.2	3.4	4.0	0.07	6.7	47	
6	15446 (16696)	647 (599)	1.92 (2.07)	0.02	1.8	20.7	20.9	4.3	4.4	0.01	1.3	20 (98)	179
	16495	606	2.05	0.09	3.5	14.9	16.4	3.1	3.4	0.05	3.5	49	
	17839	561	2.21	0.07	3.9	14.6	15.6	3.0	3.3	0.03	3.3	29	
	24175 (25809)	414 (387)	2.99 (3.20)	0.07	2.6	10.8	11.9	2.3	2.5	0.04	5.1	9 (81)	
	25194	397	3.12	0.12	3.4	13.7	15.1	2.9	3.1	0.04	5.2	17	
	26466	378	3.28	0.45	6.1	13.7	18.2	2.9	3.8	0.12	8.7	55	

[a] In butyronitrile at 77 K; observed absorption maxima, maxima for Gaussian fitting functions for $[5][PF_6]_2$ and $[6][PF_6]_2$ in parentheses. Data in all subsequent columns relate to fitted curves if used. [b] For $[3][PF_6]_2$ and $[4][PF_6]_2$, obtained from $(4.32 \times 10^{-9}\ M\ cm^2)A$ where A is the numerically integrated area under the absorption peak; for $[5][PF_6]_2$ and $[6][PF_6]_2$, obtained from $(4.60 \times 10^{-9}\ M\ cm^2)\varepsilon_{max} \times fw_{1/2}$ where ε_{max} is the maximal molar extinction coefficient and $fw_{1/2}$ is the full width at half-height (in wavenumbers). [c] Calculated using eq 2. [d] Calculated from $f_{int}\Delta\mu_{12}$ using $f_{int} = 1.33$. [e] Calculated from eq 1. [f] Delocalized electron-transfer distance calculated from $\Delta\mu_{12}/e$. [g] Effective (localized) electron-transfer distance calculated from $\Delta\mu_{ab}/e$. [h] Calculated from eq 3. [i] Calculated from eq 4. [j] Calculated from eq 5; the separate totals for the MLCT and ILCT bands are shown in parentheses.

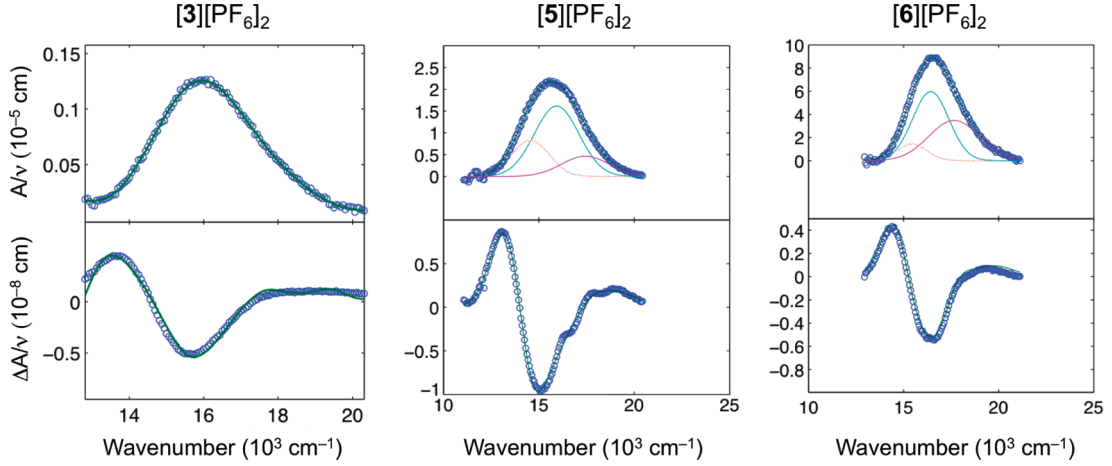

Figure 9. Electronic absorption spectra and calculated fits in the MLCT region for salts $[3][PF_6]_2$, $[5][PF_6]_2$, and $[6][PF_6]_2$ in external electric fields of 5.36, 5.26, and $5.36 \times 10^7\ V\ m^{-1}$, respectively. Top panel: absorption spectrum illustrating Gaussian curves used in data fitting for $[5][PF_6]_2$ and $[6][PF_6]_2$; bottom panel: electroabsorption spectrum, experimental (blue), and fits (green) according to the Liptay equation.[34a]

dx.doi.org/10.1021/om200604f |*Organometallics* 2011, 30, 5731–5743

$[\mathbf{5}][PF_6]_2$, and $[\mathbf{6}][PF_6]_2$ are shown in Figure 9, while the other spectra are included in the Supporting Information (Figures S6 and S7).

The MLCT and ILCT bands of $[\mathbf{3}-\mathbf{6}][PF_6]_2$ show small blue shifts of 0.03−0.08 eV on moving from acetonitrile solutions to butyronitrile glasses (Tables 2 and 4), mirroring the behavior of related purely organic species.[19] The E_{max} trends observed at room temperature are also found at 77 K, i.e. increases on replacing EDQ^{2+} with PDQ^{2+}, and little or no difference between the related MS and DS species. The band intensities at 77 K (i.e., f_{os} and μ_{12}, using total values for the DS compounds) are similar for the related EDQ^{2+}/PDQ^{2+} pairs, but switching from a MS dication to its DS counterpart markedly increases f_{os} and μ_{12}. These trends correspond with those noted for the ε values at room temperature (see above).

Using averaged values for the DS compounds, the quantities $\Delta\mu_{12}$, $\Delta\mu_{ab}$, r_{12}, and r_{ab} always decrease a little on moving from an EDQ^{2+} chromophore to its PDQ^{2+} analogue, but show no clear trends on changing from a MS dication to its DS counterpart. In almost all cases, the ILCT bands have smaller $\Delta\mu_{12}$, $\Delta\mu_{ab}$, r_{12}, and r_{ab} values when compared with their accompanying MLCT bands. This behavior is consistent with the assigned characters of the two types of transition, since greater distances are involved in the MLCT excitations, as noted by Barlow et al. and us previously.[10h,18] The ILCT bands always have somewhat larger values of f_{os}, μ_{12}, c_b^2, and H_{ab} when compared with the MLCT bands; these trends reflect the lower degree of π-orbital overlap and mixing inherent in the latter type of transition. The magnitudes of c_b^2 and H_{ab} decrease on moving from a MS chromophore to its DS analogue and (albeit often only slightly) on swapping PDQ^{2+} for EDQ^{2+}.

Given that the absorptions arise from ICT transitions, we have used the standard two-state model approach[43] (i.e., eq 5, corresponding with the so-called *B* or perturbation series convention)[44] to estimate β_0 values from the Stark data. The results are included in Table 4, and the total β_0 responses associated with the three fitted Gaussian components for each of the ICT bands are also quoted for $[\mathbf{5}][PF_6]_2$ and $[\mathbf{6}][PF_6]_2$. Related studies have shown that using this approach usually affords overall β_0 values similar to those obtained without using spectral deconvolution.[35] It should be noted that β_0 values cannot be derived from HRS data due to the presence of two contributing ICT bands in Fc-based chromophores, and no other direct experimental method for determining such responses exists. Therefore, Stark measurements provide a useful means to assess the intrinsic NLO responses of our new molecules. Although it is clear that these species are not simple two-state systems as a whole, the Stark-based approach allows them to be broken down into component electronic excitation processes that can be viewed as having two-state nature. This indirect analytical method includes the important benefit of completely avoiding complications due to resonance effects and, despite being only an approximation, has been shown previously to afford useful results with both 1D Fc derivatives[18] and purely organic DQ^{2+} derivatives.[19]

Two trends emerge from the estimated β_0 values. The first and most obvious is that moving from a MS chromophore to its DS analogue is associated with substantial (ca. 50%) increases in the quadratic NLO responses; this is mainly attributable to the larger μ_{12} values for the DS chromophores (see above). Second, the β_0 values for the EDQ^{2+} chromophores appear to be a little larger than those of their PDQ^{2+} analogues, but the differences are probably not significant. All of these observations are consistent with our previous studies on purely organic diquats.[19] The absence of a consistent correlation between the Stark-derived β_0 values and the HRS data (Table 3) may imply that the $(\langle\beta^2_{HRS}\rangle)^{1/2}$ value determined for $[\mathbf{6}][PF_6]_2$ is unexpectedly low, although repeated measurements with different samples of this compound gave similar results. However, given the fundamentally different nature of the Stark and HRS techniques and the type of chromophores studied, it is not necessarily surprising that the data do not correlate fully.

CONCLUSION

We have synthesized a family of new DQ^{2+}-based NLO chromophores containing one or two Fc π-ED groups. Their visible absorption spectra feature intense ILCT and MLCT bands that blue shift on extending the diquaternizing bridge ($EDQ^{2+} \rightarrow PDQ^{2+}$). Cyclic voltammograms show two reversible DQ^{2+}-based reductions, together with reversible $Fe^{III/II}$ oxidations, meaning that these species have a total of four accessible oxidation states. Single-crystal X-ray structures have been determined for three PF_6^- salts (one in two different solvated forms) and one mixed PF_6^-/OTf^- salt. Notably, compound $[\mathbf{6}][PF_6]_2$ adopts a polar packing arrangement that is expected to lead to bulk NLO activity. Attempted crystallization of $[\mathbf{4}][PF_6]_2$ afforded an unexpected cyclic dimeric complex tetracation that has been characterized crystallographically. This species is formed via a Michael reaction between the methyl and vinyl groups. HRS studies with a 1064 nm laser show relatively large β responses, with depolarization measurements revealing dominant "off-diagonal" β_{zyy} tensor components. Stark spectroscopy affords estimated β_0 values that are similar for the EDQ^{2+}/PDQ^{2+} pairs, but increase by ca. 50% on increasing the number of Fc-vinyl groups from one to two. The new chromophores reported are therefore interesting examples of species with large quadratic NLO responses that are potentially redox-switchable over multiple states by exploiting transition metal and purely organic DQ^{2+} moieties.

ASSOCIATED CONTENT

Supporting Information. Crystallographic information in CIF format; additional X-ray crystallographic details; additional information concerning salt $[\mathbf{4b}][PF_6]_4$; UV−vis spectra and data for $[\mathbf{3}-\mathbf{6}][PF_6]_2$ in acetone; additional spectra measured at 77 K in butyronitrile. This material is available free of charge via the Internet at http://pubs.acs.org.

AUTHOR INFORMATION

Corresponding Author
*E-mail: b.coe@manchester.ac.uk.

ACKNOWLEDGMENT

We thank the EPSRC for support (grants EP/E000738 and EP/D070732) and also the Fund for Scientific Research-Flanders (FWO-V, G.0312.08), the University of Leuven (GOA/2006/3), and the NSF (grant CHE-0802907, "Powering the Planet: an NSF Center for Chemical Innovation"). I.A. is a postdoctoral fellow of the FWO-V. We thank Ayele Teshome of the University of Leuven for technical assistance with the HRS measurements, and Dr Simon Teat of the Advanced Light Source at the University of California Berkeley for collecting the X-ray data for $[\mathbf{6}][PF_6][OTf]$.

REFERENCES

(1) (a) *Molecular Nonlinear Optics: Materials, Physics and Devices*; Zyss, J., Ed.; Academic Press: Boston, MA, USA, 1994. (b) *Organic Nonlinear Optical Materials (Advances in Nonlinear Optics, Vol. 1)*; Bosshard, Ch., Sutter, K., Prêtre, Ph., Hulliger, J., Flörsheimer, M., Kaatz, P., Günter, P., Eds.; *Advances in Nonlinear Optics*, Vol. 1; Gordon & Breach: Amsterdam, The Netherlands, 1995. (c) *Nonlinear Optics of Organic Molecules and Polymers*; Nalwa, H. S., Miyata, S., Eds.; CRC Press: Boca Raton, FL, USA, 1997. (d) Marder, S. R. *Chem. Commun.* **2006**, 131. (e) *Nonlinear Optical Properties of Matter: From Molecules to Condensed Phases*; Papadopoulos, M. G.; Leszczynski, J.; Sadlej, A. J., Eds.; Springer: Dordrecht, The Netherlands, 2006. (f) Kuzyk, M. G. *J. Mater. Chem.* **2009**, *19*, 7444.

(2) Recent reviews: (a) Le Bozec, H.; Renouard, T. *Eur. J. Inorg. Chem.* **2000**, 229. (b) Barlow, S.; Marder, S. R. *Chem. Commun.* **2000**, 1555. (c) Lacroix, P. G. *Eur. J. Inorg. Chem.* **2001**, 339. (d) Di Bella, S. *Chem. Soc. Rev.* **2001**, *30*, 355. (e) Goovaerts, E.; Wenseleers, W. E.; Garcia, M. H.; Cross, G. H. In *Handbook of Advanced Electronic and Photonic Materials and Devices*; Nalwa, H. S., Ed.; Academic Press: San Diego, CA, USA, 2001; Vol. 9, pp 127−191. (f) Coe, B. J. In *Comprehensive Coordination Chemistry II*; McCleverty, J. A., Meyer, T. J., Eds.; Elsevier Pergamon: Oxford, U.K., 2004; Vol. 9, pp 621−687. (g) Maury, O.; Le Bozec, H. *Acc. Chem. Res.* **2005**, *38*, 691. (h) Cariati, E.; Pizzotti, M.; Roberto, D.; Tessore, F.; Ugo, R. *Coord. Chem. Rev.* **2006**, *250*, 1210. (i) Coe, B. J. *Acc. Chem. Res.* **2006**, *39*, 383. (j) Thompson, M. E.; Djurovich, P. E.; Barlow, S.; Marder, S. In *Comprehensive Organometallic Chemistry III*; Crabtree, R. H., Mingos, D. M. P., Eds.; Elsevier: Oxford, U.K., 2006; Vol. 12, pp 101−194. (k) Zhang, C.; Song, Y.-L.; Wang, X. *Coord. Chem. Rev.* **2007**, *251*, 111. (l) Andraud, C.; Maury, O. *Eur. J. Inorg. Chem.* **2009**, 4357. (m) Di Bella, S.; Dragonetti, C.; Pizzotti, M.; Roberto, D.; Tessore, F.; Ugo, R. *Top. Organomet. Chem.* **2010**, *28*, 1.

(3) Selected examples: (a) Asselberghs, I.; Clays, K.; Persoons, A.; McDonagh, A. M.; Ward, M. D.; McCleverty, J. A. *Chem. Phys. Lett.* **2003**, *368*, 408. (b) Sporer, C.; Ratera, I.; Ruiz-Molina, D.; Zhao, Y.-X.; Vidal-Gancedo, J.; Wurst, K.; Jaitner, P.; Clays, K.; Persoons, A.; Rovira, C.; Veciana, J. *Angew. Chem., Int. Ed.* **2004**, *43*, 5266. (c) Cifuentes, M. P.; Powell, C. E.; Morrall, J. P.; McDonagh, A. M.; Lucas, N. T.; Humphrey, M. G.; Samoc, M.; Houbrechts, S.; Asselberghs, I.; Clays, K.; Persoons, A.; Isoshima, T. *J. Am. Chem. Soc.* **2006**, *128*, 10819. (d) Samoc, M.; Gauthier, N.; Cifuentes, M. P.; Paul, F.; Lapinte, C.; Humphrey, M. G. *Angew. Chem., Int. Ed.* **2006**, *45*, 7376. (e) Dalton, G. T.; Cifuentes, M. P.; Petrie, S.; Stranger, R.; Humphrey, M. G.; Samoc, M. *J. Am. Chem. Soc.* **2007**, *129*, 11882. (f) Boubekeur-Lecaque, L.; Coe, B. J.; Clays, K.; Foerier, S.; Verbiest, T.; Asselberghs, I. *J. Am. Chem. Soc.* **2008**, *130*, 3286. (g) Wahab, A.; Bhattacharya, M.; Ghosh, S.; Samuelson, A. G.; Das, P. K. *J. Phys. Chem. B* **2008**, *112*, 2842. (h) Guan, W.; Yang, G.-C.; Liu, C.-G.; Song, P.; Fang, L.; Yan, L.; Su, Z.-M. *Inorg. Chem.* **2008**, *47*, 5245. (i) Gauthier, N.; Argouarch, G.; Paul, F.; Toupet, L.; Ladjarafi, A.; Costuas, K.; Halet, J.-F.; Samoc, M.; Cifuentes, M. P.; Corkery, T. C.; Humphrey, M. G. *Chem.—Eur. J.* **2011**, *17*, 5561.

(4) (a) Clément, R.; Lacroix, P. G.; O'Hare, D.; Evans, J. *Adv. Mater.* **1994**, *6*, 794. (b) Lacroix, P. G.; Malfant, I.; Bénard, S.; Yu, P.; Rivière, E.; Nakatani, K. *Chem. Mater.* **2001**, *13*, 441. (c) Lacroix, P. G. *Chem. Mater.* **2001**, *13*, 3495. (d) Cariati, E.; Macchi, R.; Roberto, D.; Ugo, R.; Galli, S.; Casati, N.; Macchi, P.; Sironi, A.; Bogani, L.; Caneschi, A.; Gatteschi, D. *J. Am. Chem. Soc.* **2007**, *129*, 9410. (e) Train, C.; Nuida, T.; Gheorghe, R.; Gruselle, M.; Ohkoshi, S.-I. *J. Am. Chem. Soc.* **2009**, *131*, 16838. (f) Cariati, E.; Ugo, R.; Santoro, G.; Tordin, E.; Sorace, L.; Caneschi, A.; Sironi, A.; Macchi, P.; Casati, N. *Inorg. Chem.* **2010**, *49*, 10894. (g) Pinkowicz, D.; Podgajny, R.; Nitek, W.; Rams, M.; Majcher, A. M.; Nuida, T.; Ohkoshi, S.-I.; Sieklucka, B. *Chem. Mater.* **2011**, *23*, 21.

(5) Selected examples: (a) Dhenaut, C.; Ledoux, I.; Samuel, I. D. W.; Zyss, J.; Bourgault, M.; Le Bozec, H. *Nature* **1995**, *374*, 339. (b) Renouard, T.; Le Bozec, H.; Brasselet, S.; Ledoux, I.; Zyss, J. *Chem. Commun.* **1999**, 871. (c) Vance, F. W.; Hupp, J. T. *J. Am. Chem. Soc.* **1999**, *121*, 4047. (d) Le Bozec, H.; Le Bouder, T.; Maury, O.; Bondon, A.; Ledoux, I.; Deveau, S.; Zyss, J. *Adv. Mater.* **2001**, *13*, 1677. (e) Sénéchal, K.; Maury, O.; Le Bozec, H.; Ledoux, I.; Zyss, J. *J. Am. Chem. Soc.* **2002**, *124*, 4560. (f) Le Bouder, T.; Maury, O.; Bondon, O.; Costuas, K.; Amouyal, E.; Ledoux, I.; Zyss, J.; Le Bozec, H. *J. Am. Chem. Soc.* **2003**, *125*, 12284. (g) Maury, O.; Viau, L.; Sénéchal, K.; Corre, B.; Guégan, J.-P.; Renouard, T.; Ledoux, I.; Zyss, J.; Le Bozec, H. *Chem.—Eur. J.* **2004**, *10*, 4454. (h) Coe, B. J.; Harris, J. A.; Brunschwig, B. S.; Asselberghs, I.; Clays, K.; Garín, J.; Orduna, J. *J. Am. Chem. Soc.* **2005**, *127*, 13399. (i) Bidault, S.; Brasselet, S.; Zyss, J.; Maury, O.; Le Bozec, H. *J. Chem. Phys.* **2007**, *126*, 034312. (j) Kim, H. M.; Cho, B. R. *J. Mater. Chem.* **2009**, *19*, 7402.

(6) Selected examples: (a) Lin, W.-B.; Wang, Z.-Y.; Ma, L. *J. Am. Chem. Soc.* **1999**, *121*, 11249. (b) Evans, O. R.; Lin, W.-B. *Acc. Chem. Res.* **2002**, *35*, 511. (c) Liu, Y.; Li, G.; Li, X.; Cui, Y. *Angew. Chem., Int. Ed.* **2007**, *46*, 6301. (d) Liu, Y.; Xu, X.; Zheng, F.; Cui, Y. *Angew. Chem., Int. Ed.* **2008**, *47*, 4538. (e) Anthony, S. P. *Inorg. Chem. Commun.* **2008**, *11*, 791.

(7) Selected examples: (a) Marder, S. R.; Perry, J. W.; Schaefer, W. P. *Science* **1989**, *245*, 626. (b) Marder, S. R.; Perry, J. W.; Yakymyshyn, C. P. *Chem. Mater.* **1994**, *6*, 1137. (c) Sohma, S.; Takahashi, H.; Taniuchi, T.; Ito, H. *Chem. Phys.* **1999**, *245*, 359. (d) Kaino, T.; Cai, B.; Takayama, K. *Adv. Funct. Mater.* **2002**, *12*, 599. (e) Taniuchi, T.; Okada, S.; Nakanishi, H. *J. Appl. Phys.* **2004**, *95*, 5984. (f) Schneider, A.; Neis, M.; Stillhart, M.; Ruiz, B.; Khan, R. U. A.; Günter, P. *J. Opt. Soc. Am. B* **2006**, *23*, 1822.

(8) Selected examples: (a) Wortmann, R.; Krämer, P.; Glania, C.; Lebus, S.; Detzer, N. *Chem. Phys.* **1993**, *173*, 99. (b) Moylan, C. R.; Ermer, S.; Lovejoy, S. M.; McComb, I.-H.; Leung, D. S.; Wortmann, R.; Krämer, P.; Twieg, R. J. *J. Am. Chem. Soc.* **1996**, *118*, 12950. (c) Di Bella, S.; Fragalà, I.; Ledoux, I.; Diaz-Garcia, M. A.; Marks, T. J. *J. Am. Chem. Soc.* **1997**, *119*, 9550. (d) Wolff, J. J.; Längle, D.; Hillenbrand, D.; Wortmann, R.; Matschiner, R.; Glania, C.; Krämer, P. *Adv. Mater.* **1997**, *9*, 138. (e) Averseng, F.; Lacroix, P. G.; Malfant, I.; Lenoble, G.; Cassoux, P.; Nakatani, K.; Maltey-Fanton, I.; Delaire, J. A.; Aukauloo, A. *Chem. Mater.* **1999**, *11*, 995. (f) Hilton, A.; Renouard, T.; Maury, O.; Le Bozec, H.; Ledoux, I.; Zyss, J. *Chem. Commun.* **1999**, 2521. (g) Ostroverkhov, V.; Petschek, R. G.; Singer, K. D.; Twieg, R. J. *Chem. Phys. Lett.* **2001**, *340*, 109. (h) Di Bella, S.; Fragalà, I.; Ledoux, I.; Zyss, J. *Chem.—Eur. J.* **2001**, *7*, 3738. (i) Yang, M.-L.; Champagne, B. *J. Phys. Chem. A* **2003**, *107*, 3942. (j) Wortmann, R.; Lebus-Henn, S.; Reis, H.; Papadopoulos, M. G. *J. Mol. Struct. (THEOCHEM)* **2003**, *633*, 217. (k) Cui, Y.-Z.; Fang, Q.; Huang, Z.-L.; Xue, G.; Yu, W.-T.; Lei, H. *Opt. Mater.* **2005**, *27*, 1571. (l) Rigamonti, L.; Demartin, F.; Forni, A.; Righetto, S.; Pasini, A. *Inorg. Chem.* **2006**, *45*, 10976. (m) Li, H.-P.; Han, K.; Tang, G.; Shen, X.-P.; Wang, H.-T.; Huang, Z.-M.; Zhang, Z.-H.; Bai, L.; Wang, Z.-Y. *Chem. Phys. Lett.* **2007**, *444*, 80. (n) Zrig, S.; Koeckelberghs, G.; Verbiest, T.; Andrioletti, B.; Rose, E.; Persoons, A.; Asselberghs, I.; Clays, K. *J. Org. Chem.* **2007**, *72*, 5855. (o) Liu, C.-G.; Qiu, Y.-Q.; Su, Z.-M.; Yang, G.-C.; Sun, S.-L. *J. Phys. Chem. C* **2008**, *112*, 7021. (p) Li, H.-P.; Han, K.; Tang, G.; Li, M.-X.; Shen, X.-P.; Huang, Z.-M. *Mol. Phys.* **2009**, *107*, 1597. (q) Muhammad, S.; Janjua, M. R. S. A.; Su, Z.-M. *J. Phys. Chem. C* **2009**, *113*, 12551. (r) Sergeyev, S.; Didier, D.; Boitsov, V.; Teshome, A.; Asselberghs, I.; Clays, K.; Vande Velde, C. M. L.; Plaquet, A.; Champagne, B. *Chem.—Eur. J.* **2010**, *16*, 8181.

(9) Green, M. L. H.; Marder, S. R.; Thompson, M. E.; Bandy, J. A.; Bloor, D.; Kolinsky, P. V.; Jones, R. J. *Nature* **1987**, *330*, 360.

(10) Selected examples (neutral complexes): (a) Coe, B. J.; Jones, C. J.; McCleverty, J. A.; Bloor, D.; Kolinsky, P. V.; Jones, R. J. *J. Chem. Soc., Chem. Commun.* **1989**, 1485. (b) Kanis, D. R.; Ratner, M. A.; Marks, T. J. *J. Am. Chem. Soc.* **1990**, *112*, 8203. (c) Calabrese, J. C.; Cheng, L.-T.; Green, J. C.; Marder, S. R.; Tam, W. *J. Am. Chem. Soc.* **1991**, *113*, 7227. (d) Coe, B. J.; Foulon, J.-D.; Hamor, T. A.; Jones, C. J.; McCleverty, J. A.; Bloor, D.; Cross, G. H.; Axon, T. L. *J. Chem. Soc., Dalton Trans.* **1994**, 3427. (e) Blanchard-Desce, M.; Runser, C.; Fort, A.; Barzoukas, M.; Lehn, J.-M.; Bloy, V.; Alain, V. *Chem. Phys.* **1995**, *199*, 253. (f) Coe, B. J.; Hamor, T. A.; Jones, C. J.; McCleverty, J. A.; Bloor, D.; Cross, G. H.; Axon, T. L. *J. Chem. Soc., Dalton Trans.* **1995**, 673. (g) Mata, J.; Uriel, S.; Peris, E.; Llusar, R.; Houbrechts, S.; Persoons, A. *J. Organomet. Chem.* **1998**, *562*, 197. (h) Barlow, S.; Bunting, H. E.; Ringham, C.;

Green, J. C.; Bublitz, G. U.; Boxer, S. G.; Perry, J. W.; Marder, S. R. *J. Am. Chem. Soc.* **1999**, *121*, 3715. (i) Balavoine, G. G. A.; Daran, J.—C.; Iftime, G.; Lacroix, P. G.; Manoury, E.; Delaire, J. A.; Maltey-Fanton, I.; Nakatani, K.; Di Bella, S. *Organometallics* **1999**, *18*, 21. (j) Chiffre, J.; Averseng, F.; Balavoine, G. G. A.; Daran, J.—C.; Iftime, G.; Lacroix, P. G.; Manoury, E.; Nakatani, K. *Eur. J. Inorg. Chem.* **2001**, *9*, 2221. (k) Mata, J.; Peris, E.; Asselberghs, I.; Van Boxel, R.; Persoons, A. *New J. Chem.* **2001**, *25*, 299. (l) Tsuboya, N.; Hamasaki, R.; Ito, M.; Mitsuishi, M.; Miyashita, T.; Yumansoto, Y. *J. Mater. Chem.* **2003**, *13*, 511. (m) Liao, Y.; Eichinger, B. E.; Firestone, K. A.; Haller, M.; Luo, J.-D.; Kaminsky, W.; Benedict, J. B.; Reid, P. J.; Jen, A. K.-Y.; Dalton, L. R.; Robinson, B. H. *J. Am. Chem. Soc.* **2005**, *127*, 2758. (n) Janowska, I.; Zakrzewski, J.; Nakatani, K.; Palusiak, M.; Walak, M.; Scholl, H. *J. Organomet. Chem.* **2006**, *691*, 323. (o) Kinnibrugh, T. L.; Salman, S.; Getmanenko, Y. A.; Coropceanu, V.; Porter, W. W., III; Timofeeva, T. V.; Matzger, A. J.; Brédas, J.-L.; Marder, S. R.; Barlow, S. *Organometallics* **2009**, *28*, 1350.

(11) Kanis, D. R.; Ratner, M. A.; Marks, T. J. *J. Am. Chem. Soc.* **1992**, *114*, 10338.

(12) Selected examples: (a) Imahori, H.; Tamaki, K.; Araki, Y.; Sekiguchi, Y.; Ito, O.; Sakata, Y.; Fukuzumi, S. *J. Am. Chem. Soc.* **2002**, *124*, 5165. (b) Imahori, H.; Sekiguchi, Y.; Kashiwagi, Y.; Sato, T.; Araki, Y.; Ito, O.; Yamada, H.; Fukuzumi, S. *Chem.—Eur. J.* **2004**, *10*, 3184. (c) Morisue, M.; Kalita, D.; Haruta, N.; Kobuke, Y. *Chem. Commun.* **2007**, 2348. (d) Kumar, A.; Chauhan, R.; Molloy, K. C.; Kociok-Köhn, G.; Bahadur, L.; Singh, N. *Chem.—Eur. J.* **2010**, *16*, 4307.

(13) Selected examples: (a) Basurto, S.; Riant, O.; Moreno, D.; Rojo, J.; Torroba, T. *J. Org. Chem.* **2007**, *72*, 4673. (b) Kumar, A.; Menon, S. K. *J. Phys. Org. Chem.* **2009**, *22*, 661.

(14) Selected examples: (a) Nishikitani, Y.; Uchida, S.; Asano, T.; Minami, M.; Oshima, S.; Ikai, K.; Kubo, T. *J. Phys. Chem. C* **2008**, *112*, 4372. (b) Yin, X.-D.; Li, Y.-J.; Li, Y.-L.; Zhu, Y.-L.; Tang, X.-L.; Zheng., H.-Y.; Zhu, D.-B. *Tetrahedron* **2009**, *65*, 8373.

(15) Kondo, M.; Uchikawa, M.; Kume, S.; Nishihara, H. *Chem. Commun.* **2009**, 1993.

(16) Selected examples: (a) Marder, S. R.; Perry, J. W.; Schaefer, W. P.; Tiemann, B. G.; Groves, P. C.; Perry, K. J. *Proc. SPIE Int. Soc. Opt. Eng.* **1989**, *117*, 108. (b) Marder, S. R.; Perry, J. W.; Tiemann, B. G.; Schaefer, W. P. *Organometallics* **1991**, *10*, 1896. (c) Alain, V.; Fort, A.; Barzoukas, M.; Chen, C. T.; Blanchard-Desce, M.; Marder, S. R.; Perry, J. W. *Inorg. Chem. Acta* **1996**, *242*, 43. (d) Davies, D. A.; Silver, J.; Cross, G.; Thomas, P. *J. Organomet. Chem.* **2001**, *631*, 59. (e) Mata, J.; Peris, E.; Asselberghs, I.; Van Boxel, R.; Persoons, A. *New J. Chem.* **2001**, *25*, 1043. (f) Roque, K.; Barangé, F.; Balavoine, G. G. A.; Daran, J.—C.; Lacroix, P. G.; Manoury, E. *J. Organomet. Chem.* **2001**, *637—639*, 531. (g) Arbez-Gindre, C.; Steele, B. R.; Heropoulos, G. A.; Screttas, C. G.; Communal, J.-E.; Blau, W. J.; Ledoux-Rak, I. *J. Organomet. Chem.* **2005**, *690*, 1620.

(17) Selected examples: (a) Behrens, U.; Brussaard, H.; Hagenau, U.; Heck, J.; Hendrickx, E.; Körnich, J.; van der Linden, J. G. M.; Persoons, A.; Spek, A. L.; Veldman, N.; Voss, B.; Wong, H. *Chem.—Eur. J.* **1996**, *2*, 98. (b) Hagenau, U.; Heck, J.; Hendrickx, E.; Persoons, A.; Schuld, T.; Wong, H. *Inorg. Chem.* **1996**, *35*, 7863. (c) Farrell, T.; Meyer-Friedrichsen, T.; Malessa, M.; Haase, D.; Saak, W.; Asselberghs, I.; Wostyn, K.; Clays, K.; Persoons, A.; Heck, J.; Manning, A. R. *J. Chem. Soc., Dalton Trans.* **2001**, 29. (d) Hudson, R. D. A.; Manning, A. R.; Nolan, D. F.; Asselberghs, I.; Van Boxel, R.; Persoons, A.; Gallagher, J. F. *J. Organomet. Chem.* **2001**, *619*, 141. (e) Meyer-Friedrichsen, T.; Wong, H.; Prosenc, M. H.; Heck, J. *Eur. J. Inorg. Chem.* **2003**, 936.

(18) Coe, B. J.; Docherty, R. J.; Foxon, S. P.; Harper, E. C.; Helliwell, M.; Raftery, J.; Clays, K.; Franz, E.; Brunschwig, B. S. *Organometallics* **2009**, *28*, 6880.

(19) (a) Coe, B. J.; Harris, J. A.; Brunschwig, B. S.; Garín, J.; Orduna, J. *J. Am. Chem. Soc.* **2005**, *127*, 3284. (b) Coe, B. J.; Fielden, J.; Foxon, S. P.; Harris, J. A.; Helliwell, M.; Brunschwig, B. S.; Asselberghs, I.; Clays, K; Garín, J.; Orduna, J. *J. Am. Chem. Soc.* **2010**, *132*, 10498. (c) Coe, B. J.; Fielden, J.; Foxon, S. P.; Helliwell, M.; Brunschwig, B. S.; Asselberghs, I; Clays, K; Olesiak, J.; Matczyszyn, K.; Samoc, M. *J. Phys. Chem. A* **2010**, *114*, 12028.

(20) Lindner, E.; von Au, G.; Eberle, H.-J. *Chem. Ber.* **1981**, *114*, 810.

(21) (a) Hartshorn, C. M.; Maxwell, K. A.; White, P. S.; DeSimone, J. M.; Meyer, T. J. *Inorg. Chem.* **2001**, *40*, 601. (b) Gillaizeau-Gauthier, I.; Odobel, F.; Alebbi, M.; Argazzi, R.; Costa, E.; Bignozzi, C. A.; Qu, P.; Meyer, G. J. *Inorg. Chem.* **2001**, *40*, 6073.

(22) *CrysAlis RED* (Version 1.171.32.4), Oxford Diffraction Ltd.: Yarnton: Oxfordshire, U.K., 2006.

(23) (a) Altomare, A.; Burla, M. C.; Camalli, M.; Cascarano, G. L.; Giacovazzo, C.; Guagliardi, A.; Molirterni, A. G. G.; Polidori, G.; Spagna, R. *J. Appl. Crystallogr.* **1999**, *32*, 115. (b) Burla, M. C.; Caliandro, R.; Camalli, M.; Carrozzini, B.; Cascarano, G. L.; De Caro, L.; Giacovazzo, C.; Polidori, G.; Spagna, R. *J. Appl. Crystallogr.* **2005**, *38*, 381.

(24) Farrugia, L. J. *J. Appl. Crystallogr.* **1999**, *32*, 837.

(25) Sheldrick, G. M. *Acta Crystallogr., Sect. A* **1990**, *46*, 467.

(26) Sheldrick, G. M. *SHELXL 97*, Program for crystal structure refinement; University of Göttingen: Göttingen, Germany, 1997.

(27) *SHELXTL* (Version 6.10); Bruker AXS Inc.: Madison, WI, USA, 2000.

(28) (a) Clays, K.; Persoons, A. *Phys. Rev. Lett.* **1991**, *66*, 2980. (b) Clays, K.; Persoons, A. *Rev. Sci. Instrum.* **1992**, *63*, 3285. (c) Hendrickx, E.; Clays, K.; Pesoons, A.; Dehu, C.; Brédas, J.-L. *J. Am. Chem. Soc.* **1995**, *117*, 3547. (d) Hendrickx, E.; Clays, K.; Persoons, A. *Acc. Chem. Res.* **1998**, *31*, 675.

(29) Houbrechts, S.; Clays, K.; Persoons, A.; Pikramenou, Z.; Lehn, J.-M. *Chem. Phys. Lett.* **1996**, *258*, 485.

(30) Stähelin, M.; Burland, D. M.; Rice, J. E. *Chem. Phys. Lett.* **1992**, *191*, 245.

(31) Heesink, G. J. T.; Ruiter, A. G. T.; van Hulst, N. F.; Bölger, B. *Phys. Rev. Lett.* **1993**, *71*, 999.

(32) (a) Hendrickx, E.; Boutton, C.; Clays, K.; Persoons, A.; van Es, S.; Biemans, T.; Meijer, B. *Chem. Phys. Lett.* **1997**, *270*, 241. (b) Boutton, C.; Clays, K.; Persoons, A.; Wada, T.; Sasabe, H. *Chem. Phys. Lett.* **1998**, *286*, 101.

(33) (a) Shin, Y. K.; Brunschwig, B. S.; Creutz, C.; Sutin, N. *J. Phys. Chem.* **1996**, *100*, 8157. (b) Coe, B. J.; Harris, J. A.; Brunschwig, B. S. *J. Phys. Chem. A* **2002**, *106*, 897.

(34) (a) Liptay, W. In *Excited States*, Vol. 1; Lim, E. C., Ed.; Academic Press: New York, 1974; pp 129—229. (b) Bublitz, G. U.; Boxer, S. G. *Annu. Rev. Phys. Chem.* **1997**, *48*, 213. (c) Vance, F. W.; Williams, R. D.; Hupp, J. T. *Int. Rev. Phys. Chem.* **1998**, *17*, 307. (d) Brunschwig, B. S.; Creutz, C.; Sutin, N. *Coord. Chem. Rev.* **1998**, *177*, 61.

(35) Other recent examples: (a) Coe, B. J.; Foxon, S. P.; Harper, E. C.; Harris, J. A.; Helliwell, M.; Raftery, J.; Asselberghs, I.; Clays, K.; Franz, E.; Brunschwig, B. S.; Fitch, A. G. *Dyes Pigments* **2009**, *82*, 171. (b) Coe, B. J.; Foxon, S. P.; Harper, E. C.; Helliwell, M.; Raftery, J.; Swanson, C. A.; Brunschwig, B. S.; Clays, K.; Franz, E.; Garín, J.; Orduna, J.; Horton, P. N.; Hursthouse, M. B. *J. Am. Chem. Soc.* **2010**, *132*, 1706.

(36) Beer, P. D.; Kocian, O.; Mortimer, R. J. *J. Chem. Soc., Dalton Trans.* **1990**, 3283.

(37) Coe, B. J.; Curati, N. R. M.; Fitzgerald, E. C. *Synthesis* **2006**, 146.

(38) (a) Sonoda, A.; Moritani, I. *Bull. Chem. Soc. Jpn.* **1976**, *43*, 3522. (b) Turbitt, T. D.; Watts, W. E. *J. Chem. Soc., Perkin Trans. 2* **1974**, 177. (c) Khand, I. U.; Pauson, P. L. *J. Chem. Soc., Perkin Trans. 1* **1976**, 30. (d) Gupta, H. K.; Rampersad, N.; Stradiotto, M.; McGlinchey, M. J. *Organometallics* **2000**, *19*, 184. (e) Manzur, C.; Fuentealba, M.; Millán, L.; Gajardo, F.; Carrillo, D.; Mata, J. A.; Sinbandhit, S.; Hamon, P.; Hamon, J.-R.; Kahlal, S.; Saillard, J.-Y. *New. J. Chem.* **2002**, *26*, 213. (f) Harrington, L. E.; Britten, J. F.; McGlinchey, M. J. *Can. J. Chem.* **2003**, *81*, 1180. (g) Harrington, L. E.; Vargas-Baca, I.; Reginato, N.; McGlinchey, M. J. *Organometallics* **2003**, *22*, 663.

(39) Cambridge Structural Database (Version 5.30), May 2009 update, CCDC: Cambridge, UK, 2009.

(40) Jazbinšek, M.; Figi, H.; Hunziker, C.; Ruiz, B.; Kwon, S.-J.; Kwon, O.-P.; Yang, Z.; Günter, P. *Proc. SPIE—Int. Soc. Opt. Eng.* **2010**, *7774*, 77740Q–1.

(41) Vachon, J.; Bernardinelli, G.; Lacour, J. *Chem.—Eur. J.* **2010**, *16*, 2797.
(42) Kaatz, P.; Shelton, D. P. *J. Chem. Phys.* **1996**, *105*, 3918.
(43) (a) Oudar, J. L.; Chemla, D. S. *J. Chem. Phys.* **1977**, *66*, 2664. (b) Oudar, J. L. *J. Chem. Phys.* **1977**, *67*, 446.
(44) (a) Willetts, A.; Rice, J. E.; Burland, D. M.; Shelton, D. P. *J. Chem. Phys.* **1992**, *97*, 7590. (b) Luo, Y.; Ågren, H.; Jørgensen, P.; Mikkelsen, K. V. *Adv. Quantum Chem.* **1995**, *26*, 165.